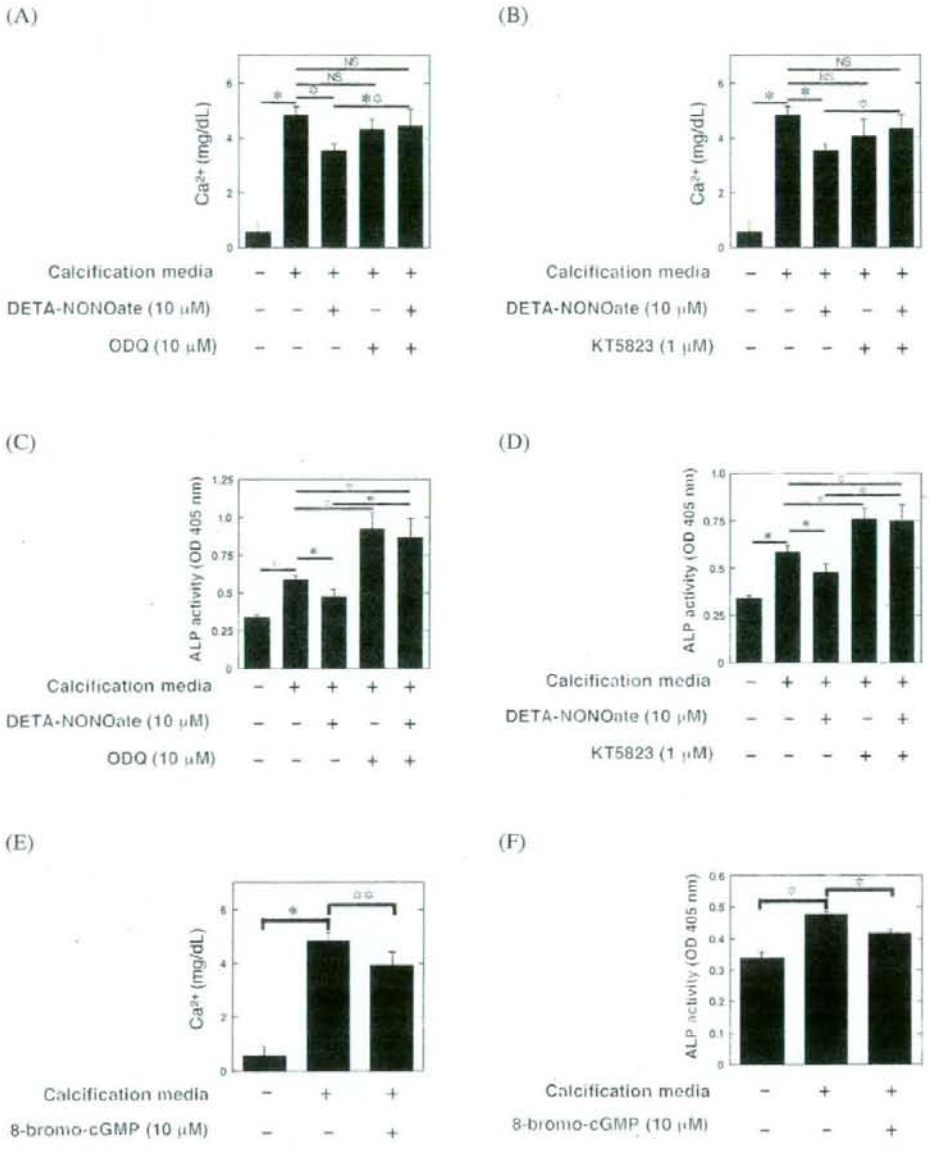

Figure 3 Nitric oxide (NO)-cGMP signalling pathway mediates vascular smooth muscle cell (VSMC) calcification. (*A*) Guanylate cyclase inhibitor ODQ blocks NO inhibition of VSMC calcification. VSMCs were grown in calcification media with 10 μM DETA-NONOate for 14 days in the presence or absence of ODQ. Then, calcium concentration in the cells was measured as described in Methods section ($n = 4$–$6 \pm$ SEM, $^*P < 0.01$, $^{**}P < 0.05$). (*B*) The PKG inhibitor KT5823 blocks NO inhibition of VSMC calcification. VSMCs were grown in calcification media with DETA-NONOate for 14 days in the presence or absence of KT5823. Mineralization was measured as above ($n = 4$–$6 \pm$ SEM, $^*P < 0.01$). (*C*) ODQ blocks NO inhibition of VSMC osteoblastic differentiation. VSMCs were grown in calcification media with 10 μM DETA-NONOate for 14 days in the presence or absence of ODQ, and ALP activity at OD 405 nm was measured ($n = 6 \pm$ SEM, $^*P < 0.01$). (*D*) KT5823 blocks NO inhibition of VSMC osteoblastic differentiation. VSMCs were grown in calcification media with DETA-NONOate for 14 days in the presence or absence of KT5823, and ALP activity at OD 405 nm was measured ($n = 6 \pm$ SEM, $^*P < 0.01$). (*E*) An analogue of cGMP, 8-bromo-cGMP, inhibits VSMC calcification. VSMCs were grown in calcification media with or without 8-bromo-cGMP for 14 days. Then, calcium concentration in the cells was measured as described in Methods section ($n = 3$–$6 \pm$ SEM, $^*P < 0.01$, $^{**}P < 0.05$). (*F*) 8-bromo-cGMP inhibits VSMC calcification. VSMCs were grown in calcification media with or without 8-bromo-cGMP for 14 days, and ALP activity at OD 405 nm was measured ($n = 3$–$6 \pm$ SEM, $^*P < 0.01$).

expression as they mature before mineralization.[22] Therefore, decreasing of ALP activity in calcifying VSMC blocks differentiation of VSMCs into osteoblastic cells. Furthermore, ALP can promote calcification by hydrolysing pyrophosphate. Thus, inhibition of ALP activity by NO may suppress calcification by a number of mechanisms. These findings suggest that NO regulates vascular calcification through inhibiting mineralization of VSMCs and differentiation of VSMCs into osteoblastic cells. On the other hand, the expression of NOS was induced in calcifying VSMCs. Our hypothesis is that

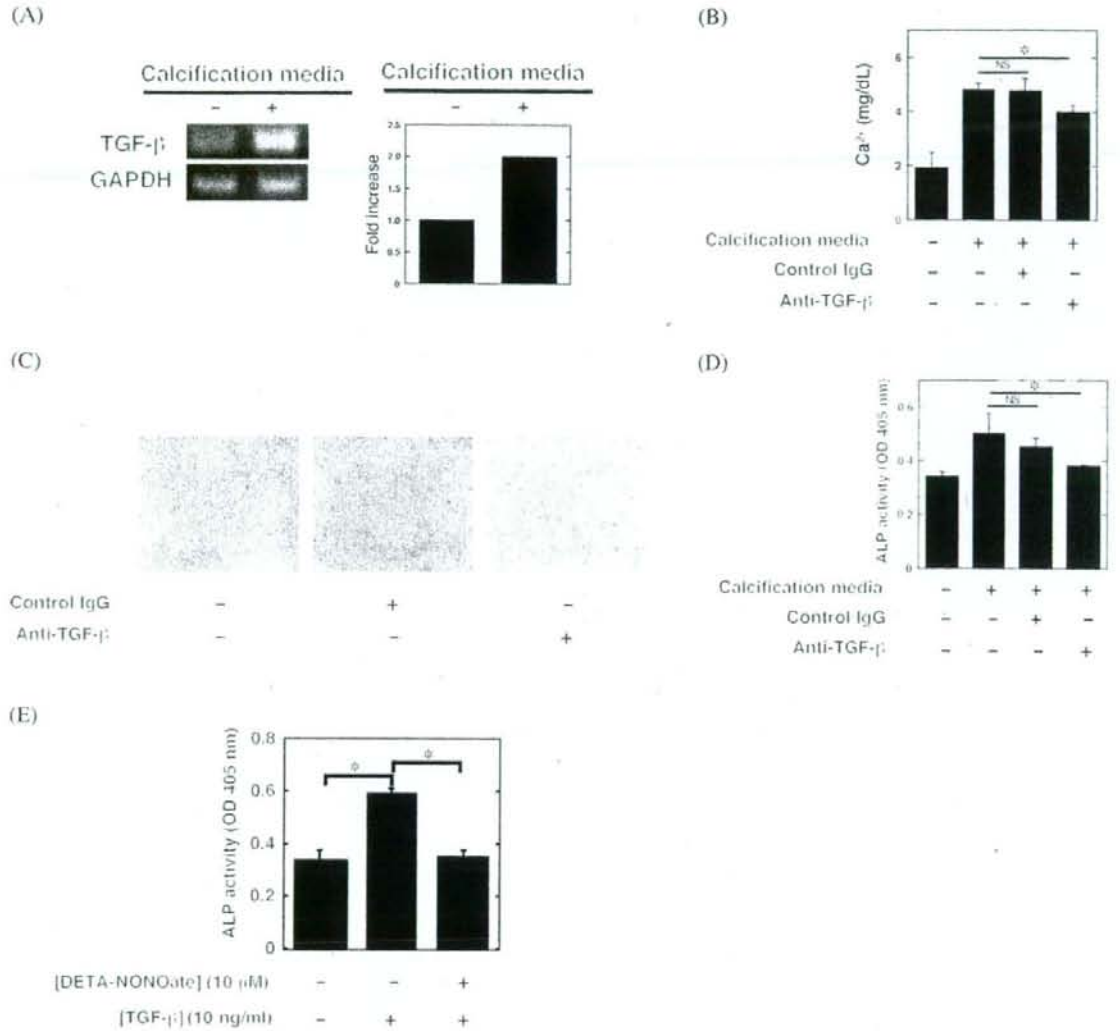

Figure 4 Transforming growth factor-β (TGF-β) induces vascular smooth muscle cell (VSMC) calcification. (*A*) TGF-β expression increases in calcifying VSMCs. VSMCs were grown for 14 days in the presence or absence of calcification medium. Then TGF-β gene expression in the cells was measured by RT-PCR. (*B*) Antibody to TGF-β1 inhibits VSMC calcification. VSMCs were grown in calcification media with various concentration of anti-TGF-β antibody or control IgG for 14 days. Then, calcium concentration in the cells was measured as described in Methods section ($n = 4$–$6 \pm$ SEM, $^*P < 0.05$). (*C*) Antibody to TGF-β1 inhibits VSMC calcification. VSMCs were grown in calcification media with various concentration of anti-TGF-β antibody or control IgG for 14 days. Then, cells were then stained with Alizarin red. (*D*) Antibody to TGF-β1 inhibits VSMC calcification. VSMCs were grown in calcification media with various concentration of anti-TGF-β antibody or control IgG for 14 days, and ALP activity at OD 405 nm was measured ($n = 4$–$6 \pm$ SEM, $^*P < 0.01$). (*E*) NO inhibits TGF-β1 induction of ALP activity. VSMCs were treated with DETA-NONOate for 2 days in the presence or absence of TGF-β1. Then ALP activity in the cells was measured ($n = 5$–$6 \pm$ SEM, $^*P < 0.01$).

calcification medium induced NOS in VSMCs, where NOS is acting in a negative feedback loop. The degree of an increase in the expression of NOS isoforms was different respectively. NOS isoforms may play a different role in the negative feedback. In addition, other studies show that calcifying vascular cells, a subpopulation of cells from the artery wall and cardiac valves, have the ability to undergo osteoblastic differentiation and mineralization, and these cells have the potential for multiple lineages similar to mesenchymal stem cells.[25] Primary VSMCs might contain these cells. These cells may also have the ability to differentiate into the other type cells. Therefore, nNOS may be expressed in calcifying vascular cells though nNOS was absent in VSMCs. Further investigation would be required to clarify the details.

How does nitric oxide inhibit vascular calcification?

NO activates soluble guanylyl cyclase to produce cGMP that is involved in the relaxant response of VSMCs. Thus, we examined the effect of the guanylate cyclase inhibitor (ODQ) and PKG inhibitor (KT5823) on calcification and osteoblastic differentiation of VSMCs following NO treatment.

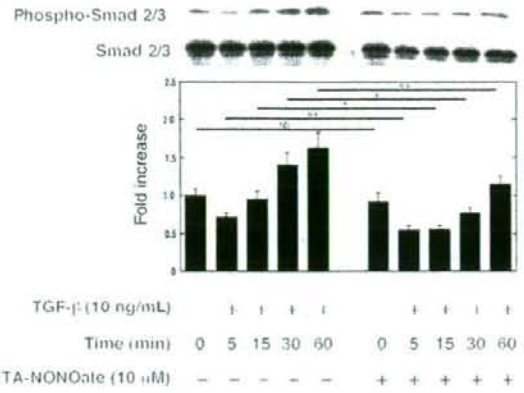

Figure 5 Nitric oxide (NO) regulates transforming growth factor-β (TGF-β) signalling in vascular smooth muscle cells (VSMCs). VSMCs were pretreated with DETA-NONOate for 60 min and then stimulated with 10 ng/mL TGF-β for the indicated periods. Phosphorylation of Smad2/3 was measured by western blot

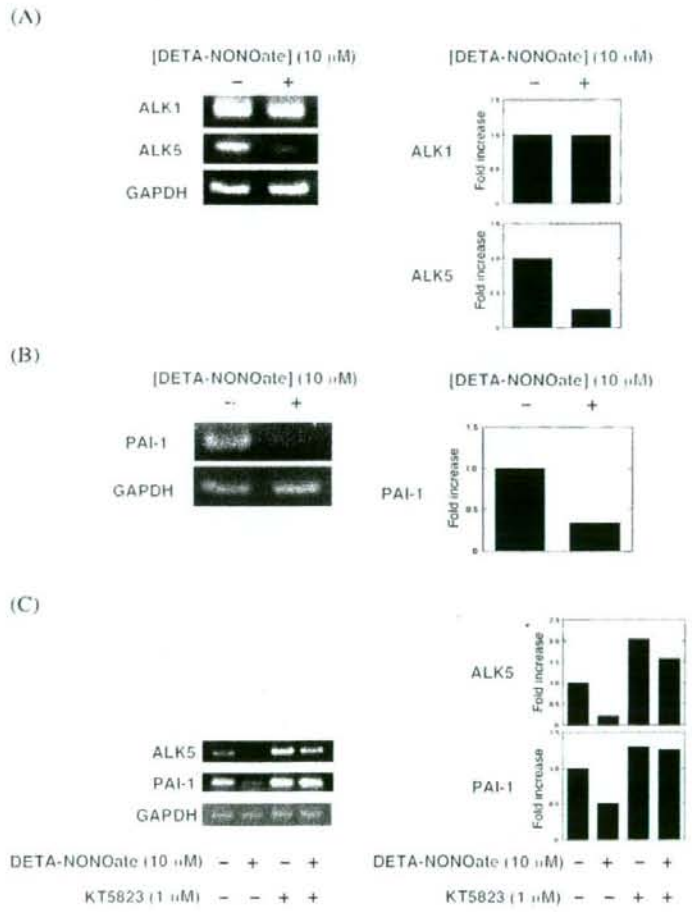

Figure 6 Nitric oxide (NO) inhibits transforming growth factor-β (TGF-β)-induced gene expression. (*A*) Effect of NO on ALK1 and ALK5 gene expression. Vascular smooth muscle cells (VSMCs) were grown in calcification media with 10 μM DETA-NONOate for 14 days. Then ALK1 and ALK5 gene expression in the cells was measured by RT–PCR. (*B*) Effect of NO on PAI-1 gene expression. Calcifying VSMCs were grown with 10 μM DETA-NONOate for 14 days. Then PAI-1 gene expression in the cells was measured by RT–PCR. (*C*) KT5823 blocks NO inhibition of ALK5 and PAI-1 gene expression. VSMCs were grown in calcification media with DETA-NONOate for 14 days in the presence or absence of KT5823, then ALK5 and PAI-1 gene expression in the cells was measured by RT–PCR. Similar results were obtained with three additional and different samples.

Inhibition of guanylate cyclase and PKG reversed the inhibitory effect of NO on vascular calcification and osteoblastic differentiation of VSMCs. Treatment of calcifying VSMCs with cGMP analogue inhibited vascular calcification and osteoblastic differentiation. These results suggest that NO regulates vascular calcification in part through the action of cGMP. However, ODQ and KT5823 did not increase VSMC calcification in the absence of NO donor. On the other hand, ODQ and KT5823 increased osteoblastic differentiation in the absence of NO donor. These data show that another possibility remains that is additional cGMP independent pathways such as S-nitrosylation of proteins by NO may also regulate calcification. We speculate as follows. First, osteoblastic differentiation is increased in VSMCs. Second, calcium accumulates in osteoblastic VSMCs. Finally, VSMC calcification is increased. cGMP/PKG signalling pathway may inhibit osteoblastic differentiation and NO may inhibit both VSMC calcification and osteoblastic differentiation. Further investigations would be required to clarify the details.

TGF-β can act as an anti-inflammatory and anti-atherogenic cytokine with a protective role in the complications of atherosclerosis. However, TGF-β also regulates vascular smooth muscle differentiation and vascular calcification.[6,15] We showed that NO reduced TGF-β signalling by decreasing expression of a TGF-β receptor ALK5, resulting in a down-regulation of TGF-β signal that induces phosphorylation of Smad2/3. TGF-β transduce signals via two distinct type I receptors, ALK1 and ALK5.[26] ALK5 induces phosphorylation of Smad2/3, while ALK1 induces phosphorylation of Smad1/5. Our results suggest that TGF-β signal via ALK5/Smad2/3 in VSMC is important for inducing vascular calcification. In addition, KT5823 reversed the inhibitory effect of NO on the ALK5 gene expression. Recently, Saura *et al.*[27] have shown that NO regulates the transcriptional responses to TGF-β by inhibiting Smad nuclear accumulation via PKG activation in ECs. This important study suggests a molecular mechanism by which NO regulates TGF-β signalling in calcification. We also found that NO regulates the TGF-β/ ALK5/Smad2/3 signalling, inhibiting TGF-β-induced gene expression of PAI-1. In addition, KT5823 reversed the inhibitory effect of NO on the PAI-1 gene expression. The fibrinolytic system plays an important role in vascular and tissue housekeeping. PAI-1 plays a key role in regulating the fibrinolytic system by serving as the primary inhibitor of t-PA and u-PA. Several groups have reported excess PAI-1 in atherosclerotic plaques in humans,[28-30] a finding that is exaggerated in type 2 diabetics.[31] These studies suggest that PAI-1 plays an important role in atherosclerosis. PAI-1 may also play an important role in vascular calcification. Inhibition of PAI-1 gene expression by NO may have an important role of calcification in VSMCs. Further investigations would be required to clarify the details.

Clinical aspects of nitric oxide and vascular calcification

NO inhibits vascular inflammation: vascular injury and atherosclerosis are more severe in knockout mice lacking eNOS or iNOS; conversely, gene therapy with NOS ameliorates arteriosclerosis.[32-35] Patients with endothelial dysfunction and defective NO synthesis is at increased risk for cardiovascular events. Our data suggest that NO and compounds that induce NO synthesis may be useful not only in inhibiting vascular inflammation, but also in preventing vascular calcification.

Supplementary material

Supplementary material is available at *Cardiovascular Research* online.

Funding

This work was supported in part by grants from Mitsui, Life Social Welfare Foundation, Aichi Cancer Research Foundation, Mitsubishi Pharma Research Foundation, Mochida Memorial Foundation for Medical and Pharmaceutical Research, and Suzuken Memorial Foundation.

Conflict of interest: All authors have no conflict of interest.

References

1. Rumberger JA, Simons DB, Fitzpatrick LA, Sheedy PF, Schwartz RS. Coronary artery calcium area by electron-beam computed tomography and coronary atherosclerotic plaque area. A histopathologic correlative study. *Circulation* 1995;92:2157-2162.
2. Abedin M, Tintut Y, Demer LL. Vascular calcification: mechanisms and clinical ramifications. *Arterioscler Thromb Vasc Biol* 2004;24:1161-1170.
3. Hruska KA, Mathew S, Saab G. Bone morphogenetic proteins in vascular calcification. *Circ Res* 2005;97:105-114.
4. Ehara S, Kobayashi Y, Yoshiyama M, Shimada K, Shimada Y, Fukuda D *et al.* Spotty calcification typifies the culprit plaque in patients with acute myocardial infarction: an intravascular ultrasound study. *Circulation* 2004;110:3424-3429.
5. Blacher J, Guérin AP, Pannier B, Marchais SJ, London GM. Arterial calcifications, arterial stiffness, and cardiovascular risk in end-stage renal disease. *Hypertension* 2001;38:938-942.
6. Watson KE, Bostrom K, Ravindranath R, Lam T, Norton B, Demer LL. TGF-beta 1 and 25-hydroxycholesterol stimulate osteoblast-like vascular cells to calcify. *J Clin Invest* 1994;93:2106-2113.
7. Otto CM, Kuusisto J, Reichenbach DD, Gown AM, O'Brien KD. Characterization of the early lesion of 'degenerative' valvular aortic stenosis. Histological and immunohistochemical studies. *Circulation* 1994;90:844-853.
8. Sato Y, Nakamura R, Satoh M, Fujishita K, Mori S, Ishida S *et al.* Thyroid hormone targets matrix Gla protein gene associated with vascular smooth muscle calcification. *Circ Res* 2005;97:550-557.
9. Shanahan CM, Cary NR, Metcalfe JC, Weissberg PL. High expression of genes for calcification-regulating proteins in human atherosclerotic plaques. *J Clin Invest* 1994;93:2393-2402.
10. Trion A, Laarse van der A. Vascular smooth muscle cells and calcification in atherosclerosis. *Am Heart J* 2004;147:808-814.
11. Ross R. The pathogenesis of atherosclerosis--an update. *N Engl J Med* 1986;314:488-500.
12. Schwartz SM, Campbell GR, Campbell JH. Replication of smooth muscle cells in vascular disease. *Circ Res* 1986;58:427-444.
13. Dhore CR, Cleutjens JP, Lutgens E, Cleutjens KB, Geusens PP, Kitslaar PJ *et al.* Differential expression of bone matrix regulatory proteins in human atherosclerotic plaques. *Arterioscler Thromb Vasc Biol* 2001;21:1998-2003.
14. Jian B, Narula N, Li QY, Mohler ER III, Levy RJ. Progression of aortic valve stenosis: TGF-beta1 is present in calcified aortic valve cusps and promotes aortic valve interstitial cell calcification via apoptosis. *Ann Thorac Surg* 2003;75:457-465.
15. Grainger DJ, Metcalfe JC, Grace AA, Mosedale DE. Transforming growth factor-beta dynamically regulates vascular smooth muscle differentiation in vivo. *J Cell Sci* 1998;111:2977-2988.
16. Nathan C, Xie Q. Nitric oxide synthases: roles, tolls, and controls. *Cell* 1994;78:915-918.
17. Stamler JS, Singel DJ, Loscalzo J. Biochemistry of nitric oxide and its redox-activated forms. *Science* 1992;258:1898-1902.

18. Dubey RK, Jackson EK, Luscher TF. Nitric oxide inhibits angiotensin II-induced migration of rat aortic smooth muscle cell. Role of cyclic-nucleotides and angiotensin1 receptors. *J Clin Invest* 1995;96:141-149.
19. Garg UC, Hassid A. Nitric oxide-generating vasodilators and 8-bromo-cyclic guanosine monophosphate inhibit mitogenesis and proliferation of cultured rat vascular smooth muscle cells. *J Clin Invest* 1989;83:1774-1777.
20. Ross R, Glomset J, Kariya B, Harker L. A platelet-dependent serum factor that stimulates the proliferation of arterial smooth muscle cells in vitro. *Proc Natl Acad Sci USA* 1974;71:1207-1210.
21. Tintut Y, Parhami F, Bostrom K, Jackson SM, Demer LL. cAMP stimulates osteoblast-like differentiation of calcifying vascular cells. Potential signaling pathway for vascular calcification. *J Biol Chem* 1998;273:7547-7553.
22. Stein GS, Lian J, Stein JL, Van Wijnen AJ, Montecino M. Transcriptional control of osteoblast growth and differentiation. *Physiol Rev* 1996;76:593-629.
23. Massague J. TGF-beta signal transduction. *Annu Rev Biochem* 1998;67:753-791.
24. Wrana JL, Attisano L, Wieser R, Ventura F, Massagué J. Mechanism of activation of the TGFβ receptor. *Nature* 1994;370:341-347.
25. Tintut Y, Alfonso Z, Saini T, Radcliff K, Watson K, Bostrom K *et al.* Multilineage potential of cells from the artery wall. *Circulation* 2003;108:2505-2510.
26. Goumans MJ, Valdimarsdottir G, Itoh S, Rosendahl A, Sideras P, ten Dijke P. Balancing the activation state of the endothelium via two distinct TGF-beta type I receptors. *EMBO J* 2002;21:1743-1753.
27. Saura M, Zaragoza C, Herranz B, Griera M, Diez-Marques L, Rodriguez-Puyol D *et al.* Nitric oxide regulates transforming growth factor-beta signaling in endothelial cells. *Circ Res* 2005;97:1115-1123.
28. Schneiderman J, Sawdey MS, Keeton MR, Bordin GM, Bernstein EF, Dilley RB *et al.* Increased type 1 plasminogen activator inhibitor gene expression in atherosclerotic human arteries. *Proc Natl Acad Sci USA* 1992;89:6998-7002.
29. Raghunath PN, Tomaszewski JE, Brady ST, Caron RJ, Okada SS, Barnathan ES. Plasminogen activator system in human coronary atherosclerosis. *Arterioscler Thromb Vasc Biol* 1995;15:1432-1443.
30. Lupu F, Bergonzelli GE, Heim DA, Cousin E, Genton CY, Bachmann F *et al.* Localization and production of plasminogen activator inhibitor-1 in human healthy and atherosclerotic arteries. *Arterioscler Thromb* 1993;13:1090-1100.
31. Sobel BE, Woodcock-Mitchell J, Schneider DJ, Holt RE, Marutsuka K, Gold H. Increased plasminogen activator inhibitor type 1 in coronary artery atherectomy specimens from type 2 diabetic compared with nondiabetic patients. *Circulation* 1998;97:2213-2221.
32. Dusting GJ, Macdonald PS. Endogenous nitric oxide in cardiovascular disease and transplantation. *Ann Med* 1995;27:395-406.
33. Qian Z, Gelzer-Bell R, Yang Sx SX, Cao W, Ohnishi T, Wasowska BA *et al.* Inducible nitric oxide synthase inhibition of weibel-palade body release in cardiac transplant rejection. *Circulation* 2001;104:2369-2375.
34. Knowles JW, Reddick R, Jennette JC, Shesely EG, Smithies O, Maeda N. Enhanced atherosclerosis and kidney dysfunction in eNOS(−/−) Apoe(−/−) mice are ameliorated by enalapril treatment. *J Clin Invest* 2000;105:451-458.
35. West NE, Qian H, Guzik TJ, Black E, Cai S, George SE *et al.* Nitric oxide synthase (nNOS) gene transfer modifies venous bypass graft remodeling: effects on vascular smooth muscle cell differentiation and superoxide production. *Circulation* 2001;104:1526-1532.

STEM CELLS
TISSUE-SPECIFIC STEM CELLS

A Novel Stem Cell Source for Vasculogenesis in Ischemia: Subfraction of Side Population Cells from Dental Pulp

KOICHIRO IOHARA,[a] LI ZHENG,[a] HIROAKI WAKE,[b] MASATAKA ITO,[c] JUNICHI NABEKURA,[b] HIDEAKI WAKITA,[d] HIROSHI NAKAMURA,[e] TAKESHI INTO,[a] KENJI MATSUSHITA,[a] MISAKO NAKASHIMA[a]

[a]Department of Oral Disease Research, National Institute for Longevity Sciences, National Center for Geriatrics and Gerontology, Obu, Aichi, Japan; [b]Department of Developmental Physiology, National Institute for Physiological Sciences, Okazaki, Aichi, Japan; [c]Department of Developmental Anatomy and Regenerative Medicine, National Defense Medical College, Tokorozawa, Saitama, Japan; [d]Department of Vascular Dementia Research, National Institute for Longevity Sciences, National Center for Geriatrics and Gerontology, Obu, Aichi, Japan; [e]Department of Endodontics, School of Dentistry, Aichigakuin University, Nagoya, Aichi, Japan

Key Words. Dental pulp stem cells • Side population cells • CD31 • Limb ischemia • Vasculogenesis • Angiogenesis

ABSTRACT

Cell therapy with stem cells and endothelial progenitor cells (EPCs) to stimulate vasculogenesis as a potential treatment for ischemic disease is an exciting area of research in regenerative medicine. EPCs are present in bone marrow, peripheral blood, and adipose tissue. Autologous EPCs, however, are obtained by invasive biopsy, a potentially painful procedure. An alternative approach is proposed in this investigation. Permanent and deciduous pulp tissue is easily available from teeth after extraction without ethical issues and has potential for clinical use. We isolated a highly vasculogenic subfraction of side population (SP) cells based on CD31 and CD146, from dental pulp. The $CD31^-$:$CD146^-$ SP cells, demonstrating $CD34^+$ and vascular endothelial growth factor-2 (VEGFR2)/$Flk1^+$, were similar to EPCs. These cells were distinct from the hematopoietic lineage as *CD11b*, *CD14*, and *CD45* mRNA were not expressed. They showed high proliferation and migration activities and multilineage differentiation potential including vasculogenic potential. In models of mouse hind limb ischemia, local transplantation of this subfraction of SP cells resulted in successful engraftment and an increase in the blood flow including high density of capillary formation. The transplanted cells were in proximity of the newly formed vasculature and expressed several proangiogenic factors, such as *VEGF-A*, *G-CSF*, *GM-CSF*, and *MMP3*. Conditioned medium from this subfraction showed the mitogenic and antiapoptotic activity on human umbilical vein endothelial cells. In conclusion, subfraction of SP cells from dental pulp is a new stem cell source for cell-based therapy to stimulate angiogenesis/vasculogenesis during tissue regeneration. STEM CELLS *2008;26:2408–2418*

Disclosure of potential conflicts of interest is found at the end of this article.

INTRODUCTION

The potential application of stem/progenitor cells to treat ischemia has generated genuine excitement in regenerative medicine [1, 2]. Endothelial progenitor cells (EPCs) are of utility to achieve corrective vasculogenesis to treat cardiac, cerebral, and limb ischemia. The characteristic features of EPCs are CD34-, CD133-, and vascular endothelial growth factor-2 (VEGFR2)-positive cells [3–5]. In both embryonic and adult human aorta $CD34^+$:$CD31^+$ cells differentiate into endothelial cells [6, 7]. Human adipose tissue-derived stromal-vascular fraction contains $CD34^+$:$CD31^-$ cells with potential to differentiate into endothelial cells [8].

The human dental pulp is a highly vascular tissue that is enriched in stem/progenitor cells [9–11]. The ready availability of dental pulp from teeth obtained during orthodontic treatment and extracted third molars circumvents any ethical concerns and is a definite advantage. In addition, their immunosuppressive properties [10] may be useful for allogeneic transplantation. Recent work in our laboratory identified stem/progenitor cells in porcine dental pulp by the use of fluorescent Hoechst dye 33342 to isolate side population (SP) cells [12]. The subfractionation of SP cells that were $CD34^+$:VEGFR2/Flk1$^+$ into $CD31^+$:$CD146^-$ and $CD31^-$:$CD146^-$ cells revealed distinct properties, the former dif-

Author contributions: K.I.: conception and design, provision of study material or patients, collection and/or assembly of data, data analysis and interpretation, manuscript writing, final approval of manuscript; L.Z.: provision of study material or patients, collection and/or assembly of data, data analysis and interpretation; H.W. and M.I.: provision of study material or patients, collection and/or assembly of data, data analysis and interpretation; J.N. and H.W.: provision of study material or patients; H.N.: financial support, provision of study material or patients; T.I.: provision of study material or patients; K.M.: financial support, final approval of manuscript; M.N.: conception and design, financial support, provision of study material or patients, collection and/or assembly of data, data analysis and interpretation, manuscript writing, final approval of manuscript.

Correspondence: Misako Nakashima, Ph.D., Department of Oral Disease Research, National Institute for Longevity Sciences, National Center for Geriatrics and Gerontology, Obu, Aichi 474-8522, Japan. Telephone: 0562-44-5651 ext. 5063; Fax: 0562-46-8684; e-mail: misako@nils.go.jp Received April 21, 2008; accepted for publication June 18, 2008; first published online in STEM CELLS *EXPRESS* June 26, 2008. ©AlphaMed Press 1066-5099/2008/$30.00/0 doi: 10.1634/stemcells.2008-0393

Downloaded from www.StemCells.com at Briscoe Library-Serials Department on March 22, 2009

ferentiated into endothelial cells in vitro. In addition, the CD31$^-$:CD146$^-$ SP cell subfraction caused functional revascularization of hind limb ischemia in vivo and is the topic of this investigation.

Materials and Methods

Isolation by Flow Cytometry

The primary pulp cells from porcine tooth germ were separated and labeled with Hoechst 33342 (Sigma, St. Louis, http://www.sigmaaldrich.com) as previously described [12]. Then the cells were preincubated with mouse BD Fc Block (BD Biosciences, San Jose, CA, http://www.bdbiosciences.com) for 30 minutes at 4°C to reduce nonspecific binding. The cells were further incubated with the mouse IgG1 negative control (MCA928) (AbD Serotec Ltd., Oxford, U.K., http://www.serotec.com), mouse IgG1 negative control (phycoerythrin [PE]) (MCA928PE) (AbD Serotec Ltd.), mouse IgG1 negative control (fluorescein isothiocyanate [FITC]) (MCA928FITC) (AbD Serotec Ltd.), mouse anti-porcine CD31 (PE) (LCI-4) (AbD Serotec Ltd.), and mouse anti-human CD146 (FITC) (OJ79c) (AbD Serotec Ltd.) in phosphate-buffered saline (PBS) with 20% fetal bovine serum (Invitrogen Corp., Carlsbad, CA, http://www.invitrogen.com) for 60 minutes at 4°C. Those were resuspended in HEPES buffer containing 2 μg/ml propidium iodide (Sigma). Analysis/sorting of cells was performed using a flow cytometer JSAN (Bay Bioscience, Kobe, Japan, http://www.baybio.co.jp).

Cell Cultures

We investigated the most suitable supplement of culture medium, EBM2 (Cambrex Bio Science Walkersville, Inc., Walkersville, MD, http://www.cambrex.com), including growth factors such as basic fibroblast growth factor (bFGF), insulin-like growth factor 1 (IGF1), epidermal growth factor (EGF), and vascular endothelial growth factor-A (VEGF-A) (Cambrex Bio Science, Inc.). The optimal concentration of porcine serum (JRH Biosciences, Inc., Lenexa, KS, http://www.jhbio.com) was also determined to maintain all the sorted cells, CD31$^-$:CD146$^-$ SP cells, CD31$^+$:CD146$^-$ SP cells, and CD31$^-$:CD146$^+$ SP cells. Each cell fraction was plated into 35-mm collagen type I-coated dishes (Asahi Technoglass Corp., Funabashi, Japan, http://www.atgc.co.jp) in EBM2 supplemented with suitable growth factors. Medium was changed every 4–5 days. Once cells reached 50%–60% confluence, they were detached by incubation with 0.02% EDTA at 37°C for 10 minutes and subcultured at a 1:4 dilution under the same conditions for more than 20 passages.

Expression of Cell Surface Markers

To characterize the phenotype of the CD31$^-$ SP cells and CD31$^+$ SP cells, the freshly isolated cells were double-stained with each antibody against CD146 (FITC) (OJ79c) (AbD Serotec Ltd.), CD11b (biotin) (M1/70) (BD Biosciences), CD14 (Alexa Flour 647) (TuK4) (AbD Serotec Ltd.), CD90 (Alexa Flour 647) (F15–42-1) (AbD Serotec Ltd.), CD117/c-kit (allophycocyanin [APC]) (A3C6F2) (Miltenyi Biotec, Bergisch Gladbach, Germany, http://www.miltenyibiotec.com), CD150 (FITC) (A12) (AbD Serotec Ltd.), CD271 (APC) (ME20.4–1H4) (Miltenyi Biotec) together with CD31 antibody after Hoechst 33342 labeling, and analyzed by flow cytometry. Streptavidin (PE-Cy7) (eBioscience, San Diego, http://www.ebioscience.com) was used for a secondary antibody of CD11b. In case of CD34 and VEGFR2/Flk1, the isolated CD31$^-$ SP cells and CD31$^+$ SP cells were cultured for 5 days to remove the CD31 antibody bound on the cell surface, and the expanded secondary cells were immunolabeled with antibodies against CD34 (QBEnd-10) (Immunotech, Cedex, France, http://www.beckmancoulter.com/products/pr_immunology.asp) and VEGFR2/Flk1 (30457) (Upstate, Spartanburg, SC, http://www.upstate.com), respectively, and goat anti-rabbit IgG (Alexa 488) (Molecular Probes, Eugene, OR, http://probes.invitrogen.com) as the secondary antibody.

Real-Time Reverse Transcription-Polymerase Chain Reaction Analysis for Cell Surface Markers and Stem Cell Markers

To characterize the phenotype of the cell population, total RNA was extracted from the freshly sorted CD31$^-$:CD146$^-$ SP cells and CD31$^+$:CD146$^-$ SP cells using Trizol (Invitrogen Corp.). The number of these cells was normalized to 5×10^4 cells in each experiment. First-strand cDNA syntheses were performed from total RNA by reverse transcription using the SuperScript II preamplification system (Invitrogen Corp.). Real-time reverse transcription-polymerase chain reaction (RT-PCR) amplifications were performed at 95°C for 10 seconds, 62°C for 15 seconds, and 72°C for 8 seconds using macrophage/mononuclear cell markers, *CD11b* and *CD14*, hematopoietic cell marker, *CD45*, angioblast marker, *CD133*, neuronal progenitor marker, *Sox2*, and stem cell markers, *CXCR4*, *Bcrp1*, *Stat3*, *Bmi1*, and *Tert* (supplemental online Table 1 and Iohara et al. [12]) labeled with Light Cycler-Fast Start DNA master SYBR Green I (Roche Diagnostics, Pleasanton, CA, http://www.roche-applied-science.com) in Light Cycler (Roche Diagnostics). The design of the oligonucleotide primers was based on published porcine cDNA sequences. When porcine sequences were not available, human sequences were used. The RT-PCR products were subcloned into pGEM-T Easy vector (Promega, Madison, WI, http://www.promega.com) and confirmed by sequencing based on published cDNA sequences. The expression in CD31$^-$:CD146$^-$ SP cells and CD31$^+$:CD146$^-$ SP cells was compared with porcine pulp tissue after normalizing with *β-actin*.

Proliferation and Migration Assay

To measure proliferation of CD31$^-$:CD146$^-$ SP cells compared with CD31$^+$:CD146$^-$ SP cells and CD31$^+$:CD146$^+$ SP cells, these cells at third passage at the 10^3 cells per 96 well were cultured in EBM2 supplemented with 0.2% bovine serum albumin (Sigma) and bFGF (50 ng/ml; Invitrogen Corp.), VEGF-A (50 ng/ml; Peprotech Ltd., London, http://www.peprotech.com), EGF (50 ng/ml, Invitrogen Corp.), stromal cell-derived factor 1 (SDF1; 50 ng/ml) (Acris, Hiddenhausen, Germany, http://www.acris-antibodies.com), and IGF1 (50 ng/ml; Peprotech Ltd.). Tetracolor one (10 μl) (Seikagaku Kogyo, Co., Tokyo, http://www.seikagaku.co.jp) was added to the 96-well plate, and cell numbers were measured using spectrophotometer at 450 nm absorbance at 0, 12, 24, 36, 48, and 72 hours of culture. Wells without cells served as negative controls.

To examine the migration activity of CD31$^-$:CD146$^-$ SP cells compared with CD31$^+$:CD146$^-$ SP cells and CD31$^-$:CD146$^+$ SP cells, 5×10^4 cells were seeded on PET-membrane (BD Biosciences) inserted into 24-well assembly containing EBM2 supplemented with VEGF-A (Peprotech Ltd.) at the final concentration of 0, 5, 10, and 100 ng/ml. Twenty-four hours later, cells that passed through the membrane were counted after detaching the cells from the membrane with 0.2% trypsin-0.02% EDTA. The migration activity was also examined in the culture with SDF1 (Acris) or granulocyte colony-stimulating factor (G-CSF) (Peprotech Ltd.) and compared with VEGF-A at the final concentration of 50 ng/ml.

Induced Chondrogenic, Adipogenic, Neurogenic, and Odontogenic Differentiation

The differentiation of pulp CD31$^-$:CD146$^-$ SP cells into adipogenic, chondrogenic, neurogenic, and odontoblastic cells was determined and compared with CD31$^-$:CD146$^-$ SP cells by the previously described methods [12]. Odontogenic potential in vivo was confirmed 28 days after autologous transplantation in a canine amputated model of pulp injury [13; K.I. manuscript submitted for publication]. The cells were transplanted in the form of a pellet (cellular aggregates) with collagen type I and type III after 1,1′-dioctadecyl-3,3,3′,3′-tetramethylindocarbocyanine perchlorate (DiI) labeling on the amputated pulp.

Endothelial Differentiation In Vitro

The CD31$^-$:CD146$^-$ SP cells, CD31$^+$:CD146$^-$ SP cells, and CD31$^-$:CD146$^+$ SP cells at the third to fifth passage were seeded

Downloaded from www.StemCells.com at Briscoe Library-Serials Department on March 22, 2009

on the matrigel (BD Biosciences) in EGM2. Network formation was observed after 24-hour cultivation. The paraffin-embedded sections on day 10 were observed by in situ hybridization analysis [12] using porcine *CEACAM1*, *CD146*, and *occludin* antisense probes. The DIG-labeled probes were constructed out of the plasmids after subcloning the RT-PCR products into pGEM-T Easy vector using each primer pair (supplemental online Table 2). CD31⁻; CD146⁻ SP cells were cultured for 14 days and then subcultured. The immunocytochemical analyses were performed with primary antibodies, anti-von Willebrand factor (vWF) (1:20) (H-300) (Santa-Cruz, Biotech, Santa Cruz, CA, http://www.scbt.com), anti-CD31 (1:20) (LCI-4) (AbD Serotec Ltd.), and anti-vascular endothelial (VE)-cadherin/CD144 (1:50) (123) (Acris). They were further stained with goat anti-mouse IgG-horseradish peroxidase (HRP) (Invitrogen Corp.) enhanced with TSA system rhodamine-conjugated tyramide (Invitrogen Corp.), goat anti-rabbit IgG-Alexa 568 (Invitrogen Corp.), and goat anti-rat IgG-HRP (GE Healthcare U.K. Ltd., Buckinghamshire, U.K., http://www.gehealthcare.com) enhanced with TSA system Alexa 488-conjugated tyramide (Invitrogen Corp.). The differential changes of expression were analyzed by a fluorescence microscope IX 71 (Olympus, Tokyo http://www.olympus-global.com) after counterstaining with Hoechst 33342.

To detect the endothelial function of histamine-mediated release of vWF, CD31⁻;CD146⁻ SP cells at the third passage were cultured in EGM2 for 14 days. They were further incubated with 10 μM histamine (Sigma) for 60 minutes and stained with an antibody against vWF. The uptake of acetylated-low-density lipoprotein (LDL) (Biomedical Technologies, Inc., Stoughton, MA, http://www.btiinc.com) as an index of endothelial function was examined. The cells derived from CD31⁻;CD146⁻ SP cells (10^4 cells/ml) at the third passage were cultured in EGM2 for 14 days. On day 17 and day 21, DiI-acetylated-LDL (Biomedical Technologies, Inc.) was added at the final concentration of 10 μg/ml for 2 hours.

Transplantation into Mouse Ischemic Hind Limbs

The potential of neovascularization of porcine pulp CD31⁻; CD146⁻ SP cells and CD31⁺;CD146⁻ SP cells was examined in a murine model of hind limb ischemia in 5-week-old severe combined immunodeficient mice (CB17; CLEA, Tokyo, http://www.clea-japan.com). PBS injection was also used as control. After inhalation anesthesia with isoflurane, the left proximal portion of femoral artery including the superficial and the deep branches and the distal portion of the saphenous artery were ligated as previously described [14]. After 24 hours, 100 μl of PBS with or without 1×10^6 freshly detached CD31⁻;CD146⁻ SP cells or CD31⁺;CD146⁻ SP cells at the third to fifth passage with DiI (Sigma) labeling was injected intramuscularly. Laser Doppler imaging (Perimed AB, Stockholm, Sweden, http://www.perimed.se) was performed 14 days after cell transplantation. The blood vessels were decorated with perfused FITC-conjugated dextran (Sigma). Neovascularization and engraftment of the transplanted cells into the hind limb were examined by confocal microscope using FLUO VIEW FV1000 (Olympus) instrument. Three-dimensional structures were reconstructed by METAMORPH (Molecular Devices, Sunnyvale, CA, http://www.moleculardevices.com) and IMARIS (Bitplane AG, Zurich, Switzerland, http://www.bitplane.com). Isolated muscle tissues of ischemic hind limb were fixed and serial cryotome sections (12 μm) were stained with Fluorescein Griffonia (Bandeiraea) Simplicifolia Lectin I/fluorescein-galanthus nivalis (snowdrop) lectin (20 μg/ml; Vector Laboratories, Inc., Youngstown, OH, http://www.vectorchemicals.com) to monitor the presence and localization of the transplanted cells in relation to newly formed blood vessels using a fluorescence microscope BIOREVO, BZ-9000 (KEYENCE, Osaka, Japan, http://www.keyence.co.jp). Microscopic digital images of six sections of every 120 μm were scanned in a frame composed of 500 μm × 380 μm rectangle and statistical analyses was performed using software, Dynamic cell count, BZ-HIC (KEYENCE). The experiment was repeated three times. The ultrathin sections of the hamstring muscles embedded in Epon were examined with an electron microscope (model 1010; JEOL, Tokyo, http://www.jeol.com) as previously described [15]. The cryotome sections obtained on day 7 were observed by in situ hybridization analysis [12] using porcine *G-CSF*, *granulocyte-macrophage colony-stimulating factor* (*GM-CSF*), *matrix metalloprotease* (*MMP*)*1*, *MMP3*, *VEGF-A*, and *CXCR4* antisense probes. The probes were constructed out of the plasmids after subcloning the PCR products using the same primers designed for real-time RT-PCR (supplemental online Table 1).

Analysis of Gene Expression of Cytokines and Enzymes by Real-Time RT-PCR

The mRNA expression of angiogenic (*VEGF-A*, *hepatocyte growth factor* [*HGF*]), chemotactic (*G-CSF*, *GM-CSF*, *MCP1*, *CXCL2*, *MDCF1*, *MDCF11*, *TF*), and proinflammatory (*interleukin* [*IL*]-*1α*, *IL-6*, *IL-12A*, *leukemia inhibitory factor* [*LIF*]) cytokines and matrix-degrading enzymes (*MMP1*, *MMP2*, *MMP3*, *MMP9*) and others (*Arginase I*, *Lipoprotein lipase*, *Dipeptidyl peptidase IV*, *Hyaluronan synthase 2* [*SIHAS2*], *parathyroid hormone-like hormone* [*PTHLH*], *Integrin β-like protein 1*, *GP38K*, and *Calcitonin receptor-stimulating peptide* [*CRSP*]) (supplemental online Table 1) was compared in pulp CD31⁻;CD146⁻ SP cells with those in pulp CD31⁻;CD146⁻ SP cells at third passage of culture by real-time RT-PCR. The RT-PCR products were confirmed by sequencing based on published cDNA sequences. The expression was compared with porcine pulp tissue after normalizing with *β-actin*.

Proliferation and Antiapoptotic Effect of Pulp CD31⁻;CD146⁻ SP Cell-Conditioned Medium

At 50% confluence, culture medium was switched to EBM2 and the conditioned media from CD31⁻;CD146⁻ SP cells and CD31⁻;CD146⁻ SP cells were collected 48 hours later. Human umbilical vein endothelial cells (HUVECs) (KURABO Industries, Osaka, Japan, http://www.kurabo.co.jp) were cultured in EGM2 containing 2% fetal bovine serum (FBS) for 24 hours and further in EBM2 containing 0.2% bovine serum albumin (BSA) for 24 hours. Then, the medium was changed into EBM2 containing 2% FBS supplemented with 20% of conditioned medium from pulp CD31⁻; CD146⁻ SP cells and CD31⁺;CD146⁻ SP cells. Cell numbers were measured by Tetra-color one. The proliferation effects of these conditioned media were compared with those of MMP3 (Millipore, Billerica, MA, http://www.millipore.com), VEGF-A (Peprotech Ltd.), G-CSF (Peprotech Ltd.), and GM-CSF (Peprotech Ltd.) at final concentration of 50 ng/ml. Data were expressed as means ± SD at four determinations. To assess the effect of the conditioned medium of CD31⁻;CD146⁻ SP cells on apoptosis, HUVECs at passage six or less were grown in EGM2 in 35-mm dish for 3 days and then incubated with 100 nM staurosporine (Sigma) in EBM2 supplemented with 20% of conditioned medium from CD31⁻;CD146⁻ SP cells and CD31⁻;CD146⁻ SP cells. As controls, MMP3, VEGF-A, G-CSF, and GM-CSF were added to the EBM2. After 8 hours, HUVECs were harvested, and the cell suspensions were treated with Annexin V-FITC (Roche Diagnostics) and propidium iodide for 15 minutes, and analyzed by flow cytometry. Data were expressed as means ± SD at three determinations.

Statistical Analyses

Data are reported as means ± SD. *P* values were calculated using the unpaired Student's *t* test. The number of replicates in each experiment is indicated in the figure legends.

Results

Isolation of CD31⁻; CD146⁻ SP Cells from Dental Pulp

Flow cytometric analyses of the SP cells from porcine adult pulp tissues were performed using antibodies against CD31 and CD146 to isolate further distinct subpopulations. CD31 is known to be highly expressed in endothelial progenitor cells and

Downloaded from www.StemCells.com at Briscoe Library-Serials Department on March 22, 2009

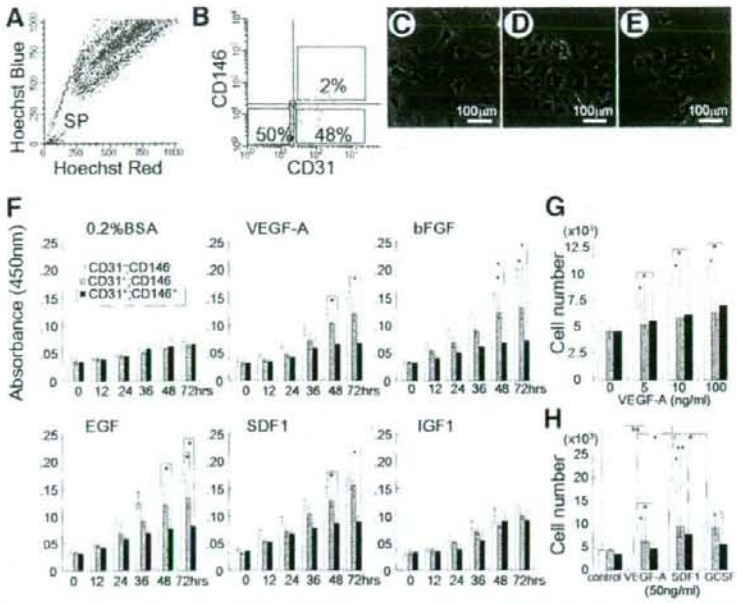

Figure 1. Isolation and comparison of proliferation and migration activities of subfractions of CD31⁻;CD146⁻, CD31⁺;CD146⁻, and CD31⁺;CD146⁺ side population (SP) cells from porcine adult dental pulp. **(A):** Flow cytometric analyses of the SP cells. Pulp cells isolated from porcine adult pulp tissues identify approximately 0.2% population with relatively lower Hoechst 33342 fluorescence (SP cells). **(B):** Isolation of further distinct populations from porcine pulp SP cells using antibodies against CD31 and CD146. CD31⁻;CD146⁻, CD31⁺;CD146⁻, and CD31⁻;CD146⁺ SP cells represented 50%, 48%, and 2%, respectively, of the total. The experiment was repeated ten times, and one representative experiment is presented. **(C, D):** Primary cell culture on day 7. **(C):** CD31⁻;CD146⁻ SP cells containing a stellate cell with long processes and a spindle-shaped cell. **(D):** Endothelial-like CD31⁺;CD146⁻ SP cells. **(E):** CD31⁺; CD146⁺ SP cells showing irregularly shaped cells with a short process. **(F):** The proliferation activity with 0.2% BSA as a control, VEGF-A, bFGF, EGF, and (IGF1) at the final concentration of 50 ng/ml. Cell numbers were determined at 0, 12, 24, 36, 48, and 72 hours of culture. Data are expressed as means ± SD at four determinations (*, $p < .01$). **(G):** The migration activity with VEGF-A at the final concentration of 0, 5, 10, and 100 ng/ml. Data were expressed as means ± SD at four determinations (*, $p < .01$). **(H):** The migration activity with VEGF-A, SDF1, and G-CSF. SDF1 induced a stronger response than VEGF-A in CD31⁻;CD146⁻ SP cells. Data were expressed as means ± SD at four determinations (*, $p < .01$; **, $p < .001$). **(F–H):** Statistical analysis was performed by the nonpaired Student's *t* test. The experiments were repeated three times and one representative experiment is presented. Abbreviations: bFGF, basic fibroblast growth factor; BSA, bovine serum albumin; EGF, epidermal growth factor; G-CSF, granulocyte colony-stimulating factor; IGF1, insulin-like growth factor 1; SDF1, stromal cell-derived factor 1; VEGF-A, vascular endothelial growth factor A.

endothelial cells and CD146, in smooth muscle cells and endothelial cells. The CD31⁻ population was devoid of CD146⁺ and represented 50% of total SP cells. The CD31⁺ population contained both CD146⁻ and CD146⁺ cells, and CD31⁺;CD146⁺ and CD31⁺;CD146⁻ represented 2% and 48% of total SP cells, respectively (Fig. 1A, 1B). The CD31⁻;CD146⁻ SP cells contained two types of cells: a stellate cell with long processes and a spindle-shaped cell. The stellate cells contained a large nucleus with nucleoli. The spindle-shaped cell was neuron-like cell with a long slender process and sparse cytoplasm (Fig. 1C). CD31⁺;CD146⁻ SP cells were endothelial-like cells, which grew clonally and were contact inhibited (Fig. 1D). CD31⁺;CD146⁺ SP cells were irregularly shaped with short processes (Fig. 1E). To maintain the phenotype of CD31⁻;CD146⁻ SP cells EBM2 supplemented with IGF1, EGF, and 10% porcine serum was used, and EBM2 with bFGF, VEGF, and 2% porcine serum was used for CD31⁺;CD146⁻ SP cells.

The single CD31⁻;CD146⁻ SP cell plated in 35-mm collagen type I-coated dish formed a colony in 8 days (data not shown), showing colony formation activity of these cells. The efficiency of attachment and growth of CD31⁻;CD146⁻ SP cells was estimated to be 8.9%, whereas for CD31⁺;CD146⁻ SP cells it was 7.7%. Limiting dilution analysis at third passage culture showed that the frequency of colony-forming unit in CD31⁻;CD146⁻ SP cells was estimated to be 80%, whereas that in CD31⁺;CD146⁻ SP cells was 30%.

Cell Surface Antigen Markers for Stem Cells

To characterize the "stemness," hematopoietic lineage, and endothelial lineage of the porcine pulp CD31⁻ SP cells and CD31⁺ SP cells, cell surface antigen markers were examined by flow cytometry and compared with CD31⁻ SP cells and CD31⁺ SP cells derived from porcine bone marrow. Markers of monocyte/macrophage origin, CD11b and CD14 were negative in pulp CD31⁻ SP cells and CD31⁺ SP cells. Few pulp CD31⁻ SP cells and CD31⁺ SP cells expressed CD90, and none expressed CD117/c-kit or CD150 (supplemental online Table 3), whereas CD31⁻ SP cells derived from porcine bone marrow expressed those at the ratio of 0%, 100%, and 1%, respectively (data not shown). Pulp CD31⁻ SP cells expressed CD34 and VEGFR2/Flk1 mRNA and proteins (supplemental online Tables 3, 4) and no *CD133* mRNA (supplemental online Table 4), suggesting that pulp CD31⁻;CD146⁻ SP cells were similar but not identical to bone marrow-derived endothelial progenitor cells. It is noteworthy that 94% of pulp CD31⁻;CD146⁻ SP cells expressed CD271/LNGFR, a marker of neuronal progenitor cells (supplemental online Table 3). *Sox2* mRNA was highly expressed in CD31⁻;CD146⁻ SP cells compared with CD31⁺;CD146⁻ SP cells (supplemental online Table 4), suggesting a neurogenic population in the former.

Expression of stem cell markers *CXCR4*, *Stat3*, *Bmi1*, and *Tert* mRNA was 8, 1.3, 1.5, and 37.5 times higher, respectively, in CD31⁻;CD146⁻ SP cells than those in CD31⁺;CD146⁻ SP cells

detected by real-time RT-PCR (supplemental online Table 4). Lack of *CD11b*, *CD14*, and *CD45* mRNA expression in CD31⁻; CD146⁻ SP cells was also confirmed (supplemental online Table 4), suggesting that they are neither of monocyte/macrophage origin nor of hematopoietic lineage.

Proliferation Activity and Chemotaxis of CD31⁻;CD146⁻ SP Cells

We first examined the proliferation activity of pulp CD31⁻; CD146⁻ SP cells and compared them with CD31⁺;CD146⁻ SP cells and CD31⁺;CD146⁺ SP cells. In the presence of 0.2% BSA without serum, all three cell populations proliferated similarly, doubled in 3 days. There is a progressive increase with time in the response to the various factors. Treatment with VEGF-A, bFGF, EGF, and SDF1 singly enhanced proliferation of CD31⁻;CD146⁻ SP cells and CD31⁺;CD146⁻ SP cells almost three times and two times more, respectively, compared with control 0.2% BSA on day 3 (Fig. 1F). IGF1 was less effective in proliferation of CD31⁻; CD146⁻ SP cells and CD31⁺;CD146⁻ SP cells but more effective in proliferation of CD31⁺;CD146⁺ SP cells compared with other growth factors (Fig. 1F).

VEGF-A (100 ng/ml) induced a chemotactic response in a dose-dependent manner in CD31⁻;CD146⁻ SP cells, and induced 1.6 and 1.4 times more strongly than that in CD31⁺; CD146⁻ SP cells and CD31⁺;CD146⁺ SP cells, respectively (Fig. 1G). SDF1 at the final concentration of 50 ng/ml also induced a two times stronger response than VEGF-A (Fig. 1H).

Multilineage Differentiation Potential Capability of SP Cells

The chondrogenic potential of CD31⁻;CD146⁻ SP cells and CD31⁺;CD146⁻ SP cells was examined in both chondrogenic and control media. The porcine pulp CD31⁻;CD146⁻ SP cells and CD31⁺;CD146⁻ SP cells from the fourth passage culture were maintained in pellet cultures for 30 days. The amount of cartilage proteoglycan stained with Alcian Blue was stronger in the pellets induced from CD31⁻;CD146⁻ SP cells compared with those from CD31⁺;CD146⁻ SP cells (Fig. 2A, 2B). The expression of chondrogenic markers *aggrecan* and *type II collagen* mRNA was much stronger in CD31⁻;CD146⁻ SP cells than in CD31⁺; CD146⁻ SP cells and SP cells 14 days after induction (data not shown). However, the expression of *type II collagen* (Fig. 2C) was similar in the two subfractions 21 days after induction. In control media there were no chondrocytes (Fig. 2C).

The adipogenic potential was examined in the third passage cultures that were cultured in adipogenic media for 28 days. Both CD31⁻;CD146⁻ SP cells and CD31⁺;CD146⁻ SP cells showed staining with oil red O (Fig. 2D, 2E), but in control media no staining was observed. Adipogenic markers *aP2* and *PPARγ* mRNA were expressed in the CD31⁻;CD146⁻ SP cells and CD31⁺;CD146⁻ SP cells on day 28 in adipogenic media (Fig. 2F).

Next, the neurogenic potential was determined. Clusters of proliferating neurospheres were more prevalent in the CD31⁻; CD146⁻ SP cells compared with CD31⁺;CD146⁻ SP cells (Fig. 2G, 2H). *Sox2* mRNA expression was similar in both groups (Fig. 2I). The neurospheres from both fractions were immunoreactive for neuromodulin 14 days after induction (Fig. 2J, 2K). The expression of neural markers *neuromodulin*, *neurofilament*, and *sodium channel, voltage-gated, type Ia (Scn1A)* mRNA was similar in the CD31⁻;CD146⁻ SP cells as that in the CD31⁺; CD146⁻ SP cells (Fig. 2L).

Finally, differentiation of CD31⁻;CD146⁻ SP cells into odontoblast lineage was examined. The mineralized matrix was stained by alizarin red in both CD31⁻;CD146⁻ SP cells and CD31⁺;CD146⁻ SP cells 28 days after induction in vitro (Fig. 2M, 2N). The DiI-labeled CD31⁻;CD146⁻ SP cells that attached to the dentinal wall in the cavity on the amputated pulp differentiated into odontoblasts and formed tubular dentin 28 days after autologous transplantation in the cavity on the canine amputated pulp in vivo (Fig. 2O–2Q). The mRNA expression of odontoblast markers, *Dspp* and *enamelysin*, was similar in CD31⁻;CD146⁻ SP cells and CD31⁺;CD146⁻ SP cells 14 days after induction in pellet culture (Fig. 2R).

Differentiation of CD31⁻;CD146⁻ SP Cells into Endothelial Cells

The endothelial differentiation potential was assessed. CD31⁻; CD146⁻ SP cells readily formed extensive networks of cords and tube-like structures as early as 12 hours (Fig. 3A), a phenotype typically associated with endothelial cells, suggesting an angioblast phenotype. On the other hand, CD31⁺;CD146⁻ SP cells and CD31⁺;CD146⁺ SP cells formed only short strands (Fig. 3B, 3C). Capillary-like structures were also observed in cells cultured in matrigel (Fig. 3D). In situ hybridization analysis showed mRNA expression of *CEACAM1* (Fig. 3E), *CD146* (Fig. 3F), and *Occludin* (Fig. 3G), markers for endothelial cells.

We also examined whether CD31⁻;CD146⁻ SP cells can differentiate into endothelial cells in monolayer culture. In the EBM2 supplemented with 2% porcine serum and 10 ng/ml VEGF-A and 10 ng/ml bFGF, endothelial marker vWF (Fig. 3H, 3K) was detected by immunocytochemistry in 3 days, whereas expression of CD31 (Fig. 3I, 3L) and VE-cadherin (Fig. 3J, 3M), a marker of more mature endothelial cells, was observed after 10 days and 21 days of culture, respectively.

Next, functional characteristics of endothelial cells induced from CD31⁻;CD146⁻ SP cells with VEGF-A were investigated. In vitro release of vWF is stimulated by histamine treatment. vWF was distributed throughout the cytoplasm prior to histamine treatment and much decreased after treatment (Fig. 3N, 3O). The uptake of acetylated-LDL in CD31⁻;CD146⁻ SP cells was high on day 21 (Fig. 3P, 3Q).

CD31⁻;CD146⁻ SP Cells Induce Functional Neovascularization in Ischemic Hind Limb

Fourteen days after transplantation of CD31⁻;CD146⁻ SP cells (Fig. 4A, 4D), the quantitative analysis of laser Doppler imaging revealed that the blood flow was significantly increased 1.3 and 1.6 times more in the ischemic hind limb compared with CD31⁺;CD146⁻ SP cells (Fig. 4B, 4D) and PBS control without cells (Fig. 4C, 4D), respectively. Capillary density was increased in the ischemic hind limb after transplantation of CD31⁻;CD146⁻ SP cells (Fig. 4E), to a greater extent compared with CD31⁺;CD146⁻ SP cells (Fig. 4F) and PBS control (Fig. 4G). Quantitative analysis using serial sections revealed that capillary density in the ischemic region transplanted with CD31⁻;CD146⁻ SP cells increased 13-fold higher than that with CD31⁺;CD146⁻ SP cells (Fig. 4H–4K). Semithin sections of the ischemic lesion of transplantation of CD31⁻;CD146⁻ SP cells (Fig. 4L) demonstrated numerous migrating cells among newly formed capillaries. Electron micrographs showed that intact capillaries with basement membrane and pericytes were surrounded by the migrating cells (Fig. 4M). Capillaries were functional with complete lumens. The migrating cells surrounding these intact capillaries were rich in cytoplasmic organelles with irregularly shaped nuclei. They were unlike the inflammatory polymorphonuclear cells or scavenging mononuclear cells (Fig. 4N). Confocal laser micrographs showed that CD31⁺;CD146⁻ SP cells were present in close proximity to the vessel (Fig. 4O, 4P), suggesting they migrated to the ischemic region and stimulated neovascularization rather than functionally incorporating into vessels (Fig.

Downloaded from www.StemCells.com at Briscoe Library-Serials Department on March 22, 2009

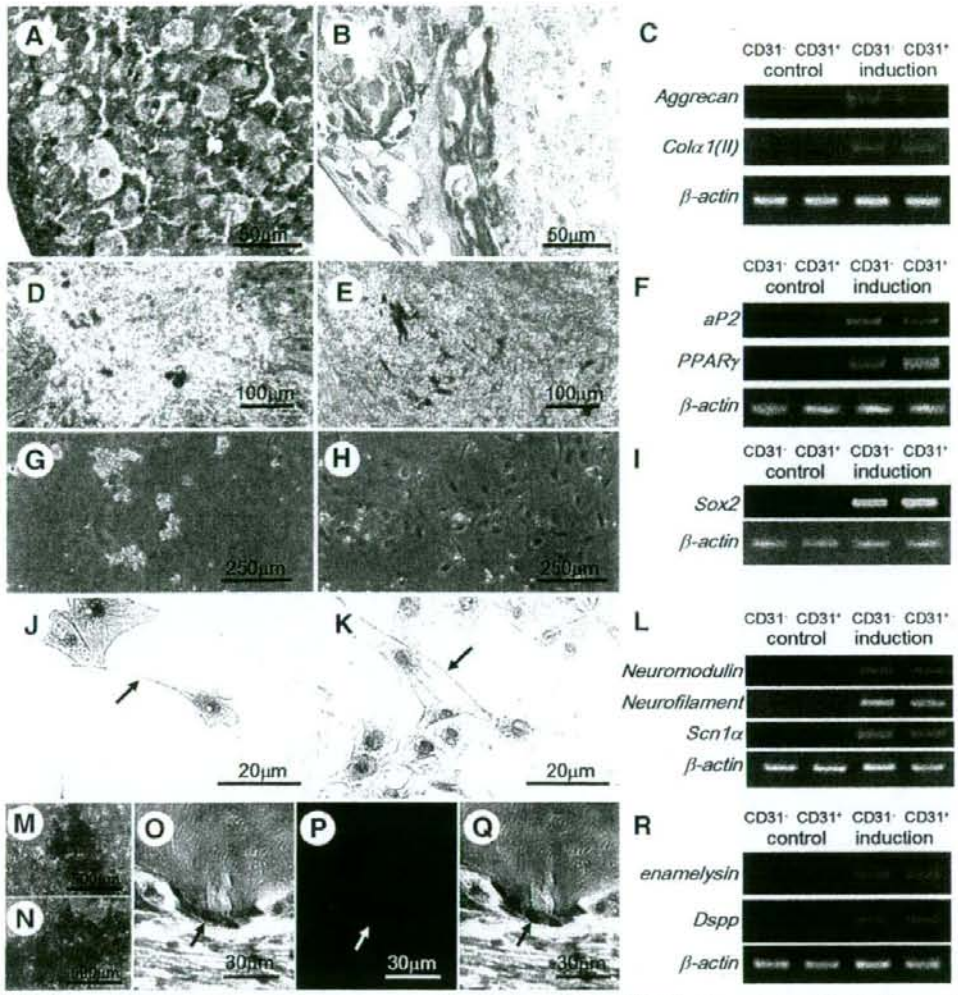

Figure 2. Multilineage differentiation potential of subfractions of CD31⁻:CD146⁻ and CD31⁺:CD146⁻ side population (SP) cells. The experiment was repeated three times, and one representative experiment is presented. **(A–C):** Chondrogenic potential. **(A, B):** Thirty days after induction of fourth passage cell populations. **(A):** CD31⁻:CD146⁻ SP cells; **(B)** CD31⁺:CD146⁻ SP cells, Alcian Blue staining. **(C):** Expression of *Aggrecan* and *Collagen α1(II)* mRNA 21 days after induction. **(D–F):** Adipogenic potential. Twenty-eight days after induction of third passage cell populations. **(D):** CD31⁻:CD146⁻ SP cells; **(E)** CD31⁺:CD146⁻ SP cells, oil red O staining. **(F):** Expression of *aP2* and *PPARγ* mRNA. **(G–I):** Neurosphere formation. Fifteen days after induction of third passage cell populations. **(G):** CD31⁻:CD146⁻ SP cells. **(H):** CD31⁺:CD146⁻ SP cells. **(I):** *Sox2* mRNA expression in the neurospheres from CD31⁻:CD146⁻ SP cells and from CD31⁺:CD146⁻ SP cells. **(J–L):** Neuronal potential. Fourteen days after induction of dissociated neurosphere cells from **(J)** CD31⁻:CD146⁻ SP cells and **(K)** CD31⁺:CD146⁻ SP cells. Immunostaining with neuromodulin. **(L):** *Neuromodulin, neurofilament,* and *sodium channel, voltage-gated, type Iα (Scn1A)* mRNA expression in CD31⁻:CD146⁻ SP cells compared with CD31⁺:CD146⁻ SP cells. **(M–R):** Odontogenic potential. **(M, N):** Twenty-eight days and **(R)** fourteen days after induction with ascorbic acid and Pi to a 4 mM final concentration in pellet culture. **(M):** CD31⁻:CD146⁻ SP cells; **(N)** CD31⁺:CD146⁻ SP cells. Alizarin red staining. **(O–Q):** Twenty-eight days after autologous transplantation of the 1,1'-dioctadecyl 3,3,3',3'-tetramethylindocarbocyanine perchlorate-labeled CD31⁻:CD146⁻ SP cells in the canine amputated pulp in vivo. Note differentiation into odontoblasts (arrows). **(O):** H&E staining. **(P):** DiI immunofluorescent image. **(Q):** Merge. **(R):** Expression of *enamelysin* and *Dspp* mRNA.

4Q). However, CD31⁻:CD146⁻ SP cells were not in close proximity of the vessels (Fig. 4Q).

Analysis of Gene Expression

The expression of angiogenic (*VEGF-A, HGF*), chemotactic (*G-CSF, GM-CSF, MCP1, CXCL2, MDC1, MDCFII, TF*), and proinflammatory (*IL-1α, IL-6, LIF*) cytokines, matrix-degrading enzymes (*MMP1, MMP3, MMP9*), and others (*Arginase I, Lipoprotein lipase, Dipeptidyl peptidase IV, Hyaluronan synthase 2, GP38K* and *CRSP*) was stronger in CD31⁻:CD146⁻ SP cells compared with CD31⁺:CD146⁻ SP cells (Table 1). *G-CSF, GM-CSF, MMP1, MMP3, VEGF-A,* and *CXCR4* were expressed in the DiI-labeled CD31⁻:CD146⁻ SP cells in the ischemic region 7 days after transplantation (Fig. 5). The conditioned medium of CD31⁻:CD146⁻ SP cells showed mitogenic (Fig. 6A) and antiapoptotic activities on HUVECs as MMP3, VEGF-A, and G-CSF (Fig. 6B). Thus, these results imply paracrine actions of proangiogenic and chemotactic cytokines in promoting neovascularization.

Downloaded from www.StemCells.com at Brigham Library-Serials Department on March 22, 2007

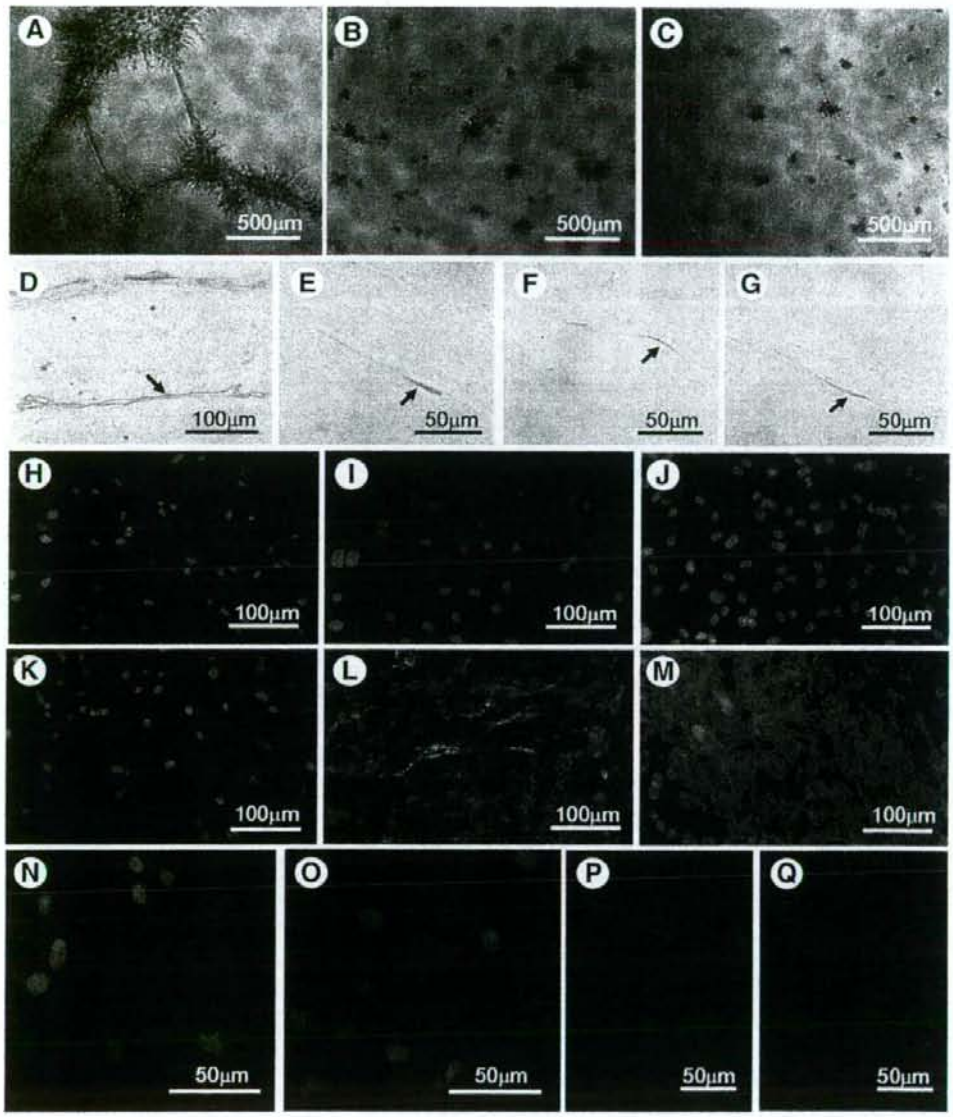

Figure 3. Differentiation of CD31⁻/CD146⁻ side population (SP) cells into endothelial cells in vitro. The experiment was repeated three times, and one representative experiment is presented. **(A–G):** The endothelial differentiation potential using the matrigel assay. **(A–C):** Twelve hours after seeding. Extensive networks of cords and tube-like structures in **(A)** CD31⁻/CD146⁻ SP cells. Smaller number of cords in **(B)** CD31⁻/CD146⁻ SP cells and **(C)** CD31⁺/CD146⁺ SP cells. **(D–G):** Capillary formation after seeding of CD31⁻/CD146⁻ SP cells at 10 days. **(D):** H&E staining. Note the capillary structure in the matrigel. In situ hybridization analysis of the markers for endothelial cells, **(E)** *CEACAM1*, **(F)** *CD146*, and **(G)** *Occludin*. Arrows show positive signals along the capillary structure. **(H–M):** Differentiation of CD31⁻/CD146⁻ SP cells into endothelial cells in monolayer culture in the presence of 2% porcine serum and 10 ng/ml vascular endothelial growth factor A and 10 ng/ml basic fibroblast growth factor. Immunocytochemistry of **(H, K)** von Willebrand factor (vWF), **(I, L)** CD31, and **(J, M)** vascular endothelial (VE)-cadherin. **(H–J):** Three days. **(K, L)** 10 days, and **(M)** 21 days of culture. Note vWF detected on day 3 and day 10; CD31, on day 10; and VE-cadherin, on day 21. **(N–Q):** Functional characteristics of endothelial cells induced from CD31⁻/CD146⁻ SP cells. **(N):** Before treatment with histamine. **(O):** After treatment with histamine, vWF was released. Uptake of acetylated-low-density lipoprotein by cells 17 days after induction **(P)** and 21 days after induction **(Q)**.

Discussion

The present investigation focused on subfractionation of SP cells from porcine dental pulp into CD31⁺; CD146⁻ and CD31⁻; CD146⁻ cells and assessment of their multilineage differentiation with special reference to vasculogenesis. There is increasing evidence of multilineage differentiation of tissue stem cells including SP cells. Previous work has demonstrated that SP cells from porcine dental pulp differentiated into adipocytes, chondrocytes,

Downloaded from www.StemCells.com at Briscoe Library-Serials Department on March 22, 2009

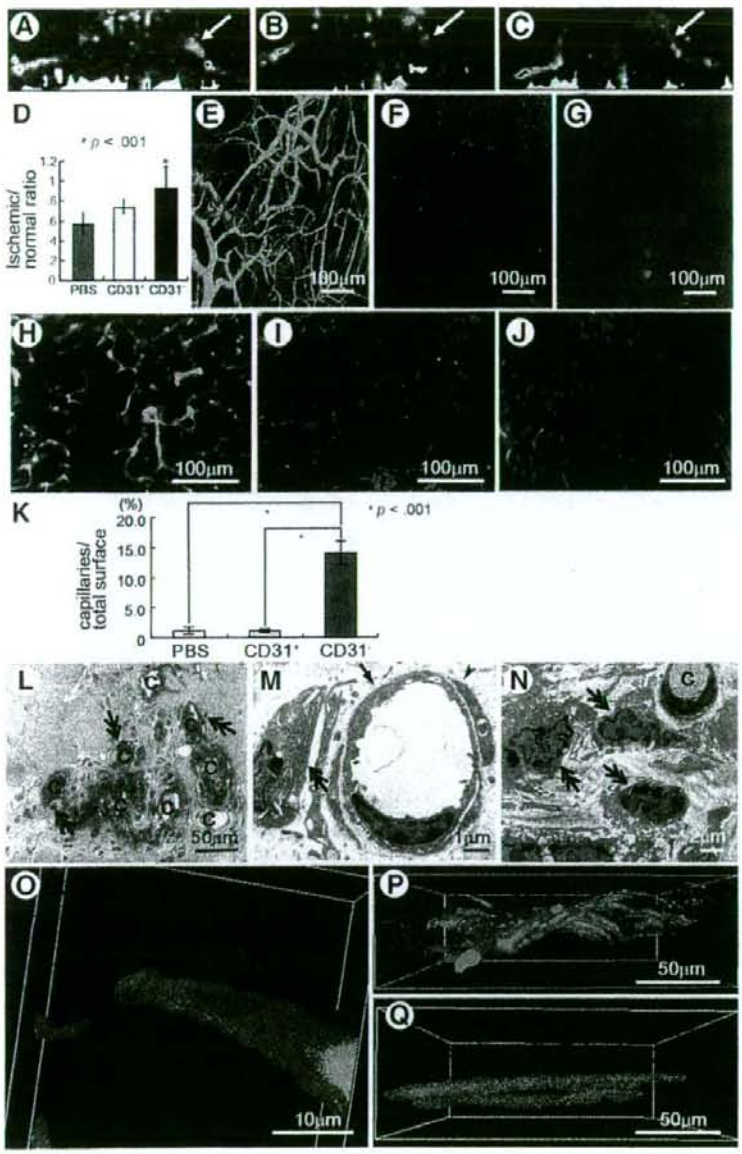

Figure 4. Neovascularization in ischemic hind limb 14 days after transplantation of CD31$^-$:CD146$^-$ side population (SP) cells compared with CD31$^-$:CD146$^-$ SP cells. **(A–C):** Laser Doppler imaging. The experiment was repeated five times, and one representative experiment is presented. **(A):** CD31$^-$:CD146$^-$ SP cells, **(B)** CD31$^+$:CD146$^-$ SP cells, and **(C)** PBS control without cells. Arrows show blood flow in the ischemic region. **(D):** Quantification of blood flow in ischemic versus control limbs obtained from five mice in each group. Statistical analysis was performed by the nonpaired Student's *t* test. **(E–G):** Confocal laser microscopic analysis after perfusion labeling with fluorescein isothiocyanate-dextran in the muscles of the ischemic hind limb. Transplantation of **(E, H)** CD31$^-$:CD146$^-$ SP cells, **(F, I)** CD31$^+$:CD146$^-$ SP cells, and **(G, J)** PBS control. **(H–J):** Stained with BS1-lectin and Hoechst 33342. **(K):** Statistical analysis using serial sections. Capillary density in the ischemic region significantly increased in transplantation of CD31$^-$:CD146$^-$ SP cells compared with PBS control and CD31$^+$:CD146$^-$ SP cells. **(L–N):** Electronmicroscopic analysis of the ischemic lesion in transplantation of CD31$^-$:CD146$^-$ SP cells. **(L):** Semithin section with toluidine blue staining showing lots of migrating cells (double arrows) among newly formed capillaries (C) in the intramuscular connective tissue. **(M):** Electronmicrogram showing intact capillaries with basement membrane (arrow) and a pericyte (arrowhead) surrounded by the migrating cells (double arrows) of the ischemic legion. **(N):** Migrating cells (double arrows) surrounding an intact capillary (C). **(O–Q):** Three-dimensional confocal laser micrograph. **(O, P):** 1,1'-dioctadecyl-3,3,3',3'-tetramethylindocarbocyanine perchlorate (DiI)-labeled CD31$^-$:CD146$^-$ SP cells present in the proximity of the vessel. **(Q):** DiI-labeled CD31$^+$:CD146$^-$ SP cells separated from the vessels. **(E–Q):** The experiment was repeated three times, and one representative experiment is presented. Abbreviation: PBS, phosphate-buffered saline.

neuronal cells, and odontoblasts [12]. Subfractionation of SP cells into CD31$^-$:CD146$^-$ and CD31$^+$:CD146$^-$ cells demonstrated that the former subfraction formed more neurospheres and expressed neurogenic marker CD271, suggesting a stronger neurogenic potential in CD31$^-$:CD146$^-$ SP cells. On the other hand, the adipogenic, chondrogenic, and odontogenic differentiation potential was similar in the two subfractions of SP cells.

It is well known that bone marrow and peripheral blood contain EPCs with properties of embryonic angioblasts with potential to differentiate into mature endothelial cells [4, 16–18]. The early angioblasts and EPCs express CD34, CD133, and VEGFR2. The expression of CD133 declines and that of CD146 increases in the differentiated endothelial cells [19, 20]. During maturation of bone marrow angioblasts to early EPCs, CD31 is expressed [21]. In human embryonic aorta [6] and human adult vascular wall [7], the endothelial progenitors are CD34$^+$ and CD31$^-$. The adipose tissue-derived stromal-vascular fraction also contains CD34$^+$:CD31$^-$ cells [8]. It is noteworthy that the porcine pulp SP subfraction, CD31$^-$:CD146$^-$ SP cells expressed CD34 and VEGFR2 as in EPCs. However, they lacked CD11b, CD14, and CD45, demonstrating that these cells are distinct from the hematopoietic lineage. In addition, it is noteworthy that pulp CD31$^-$:CD146$^-$ SP cells did not express *CD133* mRNA unlike the adipose tissue- and bone marrow-derived EPCs. Thus, the porcine pulp CD31$^-$:CD146$^-$ SP cells are similar but not identical to EPCs and expressed stem cell markers, *CXCR4*, *Stat3*, *Bmi1*, and *Tert*.

Vasculogenic potential of CD34$^+$:VEGFR2$^+$:CD133$^+$:CD90$^+$ stem cells derived from human dental pulp has been

Downloaded from www.StemCells.com at Biblos Library-Scholarly Communication on March 22, 2007

Table 1. Relative mRNA expression of cytokines and enzymes by real-time reverse transcription-polymerase chain reaction in CD31$^-$:CD146$^-$ side population (SP) cells, pulp CD31$^+$ SP cells

	CD31$^-$;CD146$^-$ SP / pulp tissue	CD31$^+$;CD146$^-$ SP / pulp tissue
VEGF-A	154.3	65.3
HGF	1.0	0.1
G-CSF	26.9	0.2
GM-CSF	1260.7	1.2
MCP1/CCL2	30.3	0.6
CXCL2	26.9	0.1
MDCF I	1243.3	21.6
MDCF II	2033.9	0.1
TF	42.2	0.8
SDF1	1.2	23.9
IL-1α	229.1	2.7
IL-6	257.8	4.5
IL-12	0.2	1.0
LIF	128.0	1.7
MMP1	3281.2	0.8
MMP2	1.4	0.7
MMP3	61.4	0.0
MMP9	1.3	0.2
Arginase I	68.1	3.6
Lipoprotein lipase	4.5	0.1
Dipeptidyl peptidase IV	1.1	0.0
SHAS2	30.7	0.3
PTHLH	0.6	0.0
Integrin, beta-like 1	12.7	0.3
GP38K	657.1	0.1
CRSP	50.2	0.1

*The value is expressed as relative expression to that in CD31$^+$; CD146$^-$ SP cells, since the pulp tissue did not express *IL-12*.

reported in the induced bone tissue after subcutaneous transplantation [22] and in myocardial infarction [23]. In the present study, the functional ability of neovascularization of CD31$^-$; CD146$^-$ SP cells was determined and demonstrated to form extensive networks of cords and tube-like structures on matrigel. On the other hand, CD31$^+$;CD146$^-$ SP cells were feeble in cord formation. Treatment of CD31$^-$:CD146$^-$ SP cells with VEGF-A and bFGF resulted in VE-cadherin expression, histamine-induced vWF release, and uptake of acetylated-LDL, all hallmarks of endothelial differentiation. In addition, CD31$^-$:CD146$^-$ SP cells exhibited neovascularization in the mouse hind limb ischemia model.

After injury, endothelial cells increase expression of VEGF, which induces SDF1 in the perivascular fibroblasts. SDF1 mobilizes CXCR4-positive cells to the perivascular site where they act in a paracrine fashion to enhance proliferation of resident endothelial cells [24]. The regeneration potential for dentin-pulp complex in response to pulp injury may be attributed to pulp stem/progenitor cells migrating from perivascular region in the pulp tissue deeper from the injured site [25]. The proangiogenic signals such as VEGF released from injured dental pulp cells [26] and endothelial cells [27] or from carious dentin [28] provide chemotactic signals to recruit pulp stem/progenitor cells in pulp tissue. CD31$^-$:CD146$^-$ SP cells showed higher expression of *CXCR4* compared with CD31$^-$:CD146$^+$ SP cells. CD31$^-$:CD146$^-$ SP cells were in proximity of vessel and close to neighboring cells expressing *SDF1* (data not shown). CD31$^+$:CD146$^-$ SP cells were at a distance from it in the ischemia model. CD31$^-$:CD146$^-$ SP cells exhibits high migration activity by VEGF and SDF1 compared with CD31$^+$; CD146$^-$ SP cells in the chemotaxis experiment. These results imply SDF1/CXCR4 system for migration of pulp CD31$^-$; CD146$^-$ SP cells in the ischemic region.

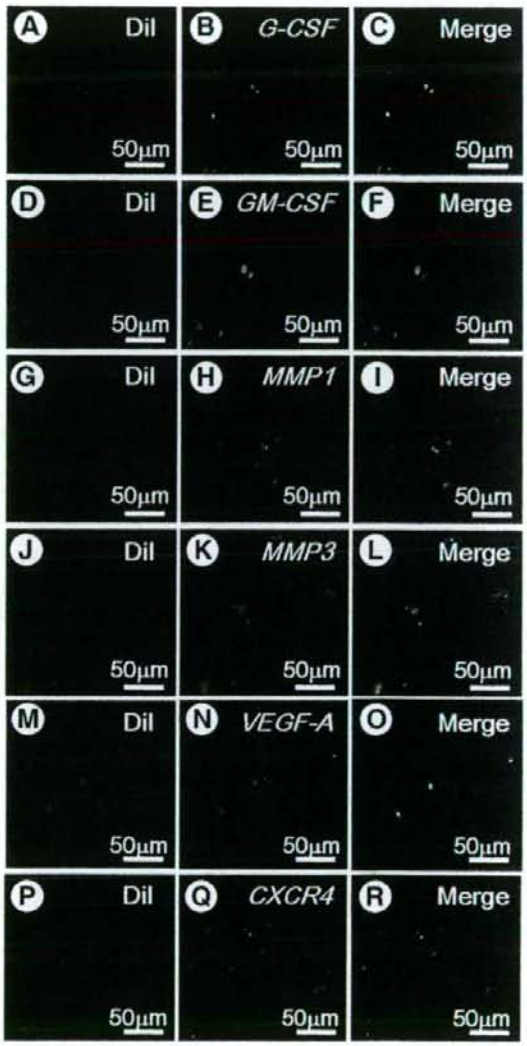

Figure 5. Analysis of gene expression by in situ hybridization. The experiment was repeated three times, and one representative experiment is presented. **(A–C)** *G-CSF*, **(D–F)** *GM-CSF*, **(G–I)** *MMP1*, **(J–L)** *MMP3*, **(M–O)** *VEGF-A*, and **(P–R)** *CXCR4* mRNA are expressed in the 1,1′-dioctadecyl-3,3,3′,3′-tetramethylindocarboeyanine perchlorate (DiI)-labeled CD31$^-$:CD146$^-$ side population (SP) cells transplanted in the mouse hind limb ischemic region 7 days after transplantation.

It is important to note these CD31$^-$:CD146$^-$ SP cells compared with CD31$^+$:CD146$^-$ SP cells expressed more *VEGF-A*, *G-CSF*, and *GM-CSF*. G-CSF promotes endothelial migration and tubule formation in vitro, and local injection of G-CSF effectively augments ischemia-induced angiogenesis in vivo [29]. GM-CSF induces vascular proliferation and improves blood flow in coronary artery disease and cerebral artery occlusion [30–32]. MMPs are involved in degrading extracellular and basement membrane structures, allowing endothelial migration to occur. MMPs also promote the release of extracellular matrix-bound cytokines, such as VEGF, which can promote proliferation of EPCs and endothelial cells and

Downloaded from www.StemCells.com at Briscoe Library-Serials Department on March 22, 2009

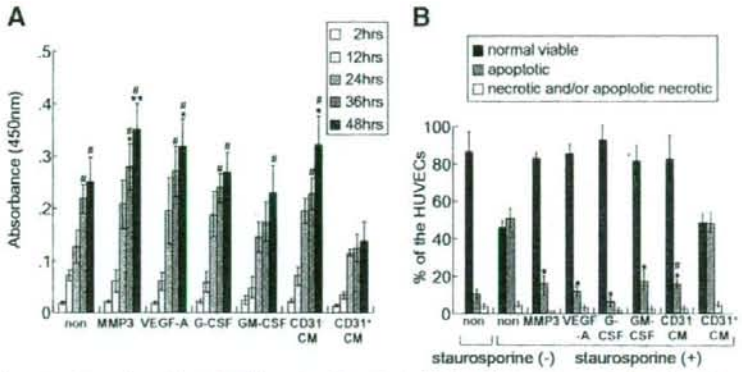

Figure 6. The mitogenic and antiapoptotic activity of conditioned medium of pulp CD31$^+$;CD146$^-$ side population (SP) cells on endothelium. Data were expressed as means ± SD at four determinations. The experiment was repeated three times, and one representative experiment is presented. Statistical analysis was performed by the nonpaired Student's *t* test. (**A**): The proliferation activity of the CM of CD31$^+$;CD146$^-$ SP cells compared with MMP3, VEGF-A, G-CSF, and GM-CSF and CM of CD31$^+$;CD146$^-$ SP cells on human umbilical vein endothelial cells (HUVECs) at 2, 12, 24, 36, and 48 hours of culture with Tetra-color one. Note the significant increase with CM of CD31$^-$;CD146$^-$ SP cells as well as those with cytokines compared with CM of CD31$^+$;CD146$^-$ SP cells (*, $p < .01$) at 36 and 48 hours. #, $p < .01$; ‡, $p < .05$ versus control. (**B**): The relative percentages of viable, apoptotic, and "apoptotic necrotic" or necrotic HUVECs analyzed by flow cytometry. In the presence of 100 nM staurosporine, the CM of pulp CD31$^-$;CD146$^-$ SP cells had significant antiapoptotic effect as MMP3, VEGF-A, G-CSF, and GM-CSF compared with control (*, $p < .01$), and higher effect compared with the CM of pulp CD31$^+$;CD146$^-$ SP cells (*, $p < .01$). Abbreviations: CM, conditioned medium; G-CSF, granulocyte colony-stimulating factor; GM-CSF, granulocyte-macrophage colony-stimulating factor; MMP3, matrix metalloprotease 3; VEGF-A, vascular endothelial growth factor A.

regulate angiogenesis [33–36]. The higher gene and protein expression of MMP3 by pulp-derived CD31$^-$;CD146$^-$ SP cells compared with CD31$^+$;CD146$^-$ SP cells is noteworthy and may explain the anticipated invasive behavior during endothelial migration [33, 37, 38]. The conditioned medium of pulp-derived CD31$^-$;CD146$^-$ SP cells enhanced proliferation and survival rate of HUVECs, suggesting the paracrine role of CD31$^-$;CD146$^-$ SP cells on local vascular cells to create a permissive environment that enables rapid revascularization, proliferation, and survival of damaged cells [39, 40]. The isolation of EPCs from bone marrow, umbilical cord blood, peripheral blood, and adipose tissue is documented. To this list of sources of EPCs now dental pulp tissue-derived CD31$^-$;CD146$^-$ SP cells can be added. It provides advantages for clinical use, since autologous pulp tissue is easily available from useless teeth after extraction with no ethical issues.

Conclusion

Dental pulp-derived CD31$^-$;CD146$^-$ subfraction of SP cells is vasculogenic, and may induce vasculogenesis in vivo in the amputated pulp model. We are aware of the potential clinical utility to ameliorate ischemic disease and pulp regeneration in the cell therapy for endodontics and operative dentistry.

Acknowledgments

The authors are grateful to Drs. N. Shibata and K. Adachi for their help. This work was supported by grants from the Collaborative Development of Innovative Seeds, Potentiality verification stage from Japan Science and Technology Agency; grants-in-aid for Scientific Research from the Ministry of Education, Science, Sports and Culture, Japan: number 17390509 (M.N.), number 19659499 (M.N.), and number 19791418 (K.I.); the Mitsubishi Pharma Research Foundation (2007, M.N.); the Japan Health Foundation (2007, M.N.); and Aichigakuin University High-Tech Research Center "Project for Private Universities: matching fund subsidy" from MEXT (Ministry of Education, Culture, Sports, Science and Technology), 2003–2007.

Disclosure of Potential Conflicts of Interest

The authors indicate no potential conflicts of interest.

References

1 Takakeslu T, Kalka C, Masuda H et al. Ischemia- and cytokine-induced mobilization of bone marrow-derived endothelial progenitor cells for neovascularization. Nature Med 1999;5:434–438.
2 Crosby JR, Kaminski WE, Schatteman G et al. Endothelial cells of hematopoietic origin make a significant contribution to adult blood vessel formation. Circ Res 2000;87:728–730.
3 Gehling UM, Ergun S, Schumacher U et al. In vitro differentiation of endothelial cells from AC133-positive progenitor cells. Blood 2000;95:3106–3112.
4 Peichev M, Naiyer AJ, Pereira D et al. Expression of VEGFR-2 and AC133 by circulating human CD34(+) cells identifies a population of functional endothelial precursors. Blood 2000;95:952–958.
5 Taguchi A, Soma T, Tanaka H et al. Administration of CD34+ cells after stroke enhances neurogenesis via angiogenesis in a mouse model. J Clin Invest 2004;114:330–338.
6 Alessandri G, Girelli M, Taccagni G et al. Human vasculogenesis ex vivo: Embryonal aorta as a tool for isolation of endothelial cell progenitors. Lab Invest 2001;81:875–885.
7 Zengin E, Chalajour F, Gehling UM et al. Vascular wall resident progenitor cells: A source for postnatal vasculogenesis. Development 2006;133:1543–1551.
8 Miranville A, Heeschen C, Sengenes C et al. Improvement of postnatal neovascularization by human adipose tissue-derived stem cells. Circulation 2004;110:349–355.
9 Gronthos S, Brahim J, Li W. Stem cell properties of human dental pulp stem cells. J Dent Res 2002;81:531–535.
10 Pierdomenico L, Bonsi L, Calvitti M et al. Multipotent mesenchymal stem cells with immunosuppressive activity can be easily isolated from dental pulp. Transplantation 2005;27:836–842.
11 Papaccio G, Graziano A, d'Aquino R, et al. Long-term cryopreservation

Downloaded from www.StemCells.com at Briscoe Library-Serials Department on March 22, 2009

of dental pulp stem cells (SBP-DPSCs) and their differentiated osteoblasts: A cell source for tissue repair. J Cell Physiol 2006;208:319–325.
12 Iohara K, Zheng L, Ito M et al. Side population cells isolated from porcine dental pulp tissue with self-renewal and multipotency for dentinogenesis, chondrogenesis, adipogenesis, and neurogenesis. STEM CELLS 2006;24:2493–2503.
13 Nakashima M. Dentin induction by implants of autolyzed antigen-extracted allogeneic dentin on amputated pulps of dogs. Endod Dent Traumatol 1989;5:279–286.
14 Couffinhal T, Silver M, Zheng LP et al. Mouse model of angiogenesis. Am J Pathol 1998;152:1667–1679.
15 Ito M, Yoshioka M. Regression of the hyaloid vessels and pupillary membrane of the mouse. Anat Embryol 1999;200:403–411.
16 Asahara T, Murohara T, Sullivan A et al. Isolation of putative progenitor endothelial cells for angiogenesis. Science 1997;275:964–967.
17 Garmy-Susini B, Varner JA. Circulating endothelial progenitor cells. Br J Cancer 2005;93:855–858.
18 Reyes M, Dudek A, Jahagirdar B et al. Origin of endothelial progenitors in human postnatal bone marrow. J Clin Invest 2002;109:337–346.
19 Bardin N, Frances V, Lesaule G et al. Identification of the S-Endo 1 endothelial-associated antigen. Biochem Biophys Res Commun 1996; 218:210–216.
20 Bardin N, George F, Mutin M et al. S-Endo 1, a pan-endothelial monoclonal antibody recognizing a novel human endothelial antigen. Tissue Antigens 1996;48:531–539.
21 Hristov M, Weber C. Endothelial progenitor cells: Characterization, pathophysiology, and possible clinical relevance. J Cell Mol Med 2004; 8:498–508.
22 d'Aquino R, Graziano A, Sampaolesi M et al. Human postnatal dental pulp cells co-differentiate into osteoblasts and endotheliocytes: A pivotal synergy leading to adult bone tissue formation. Cell Death Differ 2007; 14:1162–1171.
23 Gandia C, Arminan A, Garcia-Verdugo JM et al. Human dental pulp stem cells improve left ventricular function, induce angiogenesis, and reduce infarct size in rat with acute myocardial infarction. STEM CELLS 2008;26:638–645.
24 Grunewald M, Avraham I, Dor Y et al. VEGF-induced adult neovascularization: Recruitment, retention, and role of accessory cells. Cell 2006; 124:175–189.
25 Yamamura T. Differentiation of pulpal cells and inductive influences of various matrices with reference to pulpal wound healing. J Dent Res 1985;64:530–540.
26 Tran-Hung L, Mathieu S, About I. Role of human pulp fibroblasts in angiogenesis. J Dent Res 2006;85:819–823.
27 Mathieu S, El-Battari A, Dejou J et al. Role of injured endothelial cells in the recruitment of human pulp cells. Arch Oral Biol 2005;50:109–113.
28 Roberts-Clark DJ, Smith AJ. Angiogenic growth factors in human dentine matrix. Arch Oral Biol 2000;45:1013–1016.
29 Lee M, Aoki M, Kondo T et al. Therapeutic angiogenesis with intramuscular injection of low-dose recombinant granulocyte-colony stimulating factor. Arterioscler Thromb Vasc Biol 2005;25:2535–2541.
30 Seiler C, Pohl T, Wustmann K et al. Promotion of collateral growth by granulocyte-macrophage colony-stimulating factor in patients with coronary artery disease: A randomized, double-blind, placebo-controlled study. Circulation 2001;104:2012–2017.
31 Buschmann IR, Busch HJ, Mies G et al. Therapeutic induction of arteriogenesis in hypoperfused rat brain via granulocyte-macrophage colony-stimulating factor. Circulation 2003;108:610–615.
32 Schneeloch E, Mies G, Busch HJ et al. Granulocyte-macrophage colony-stimulating factor-induced arteriogenesis reduces energy failure in hemodynamic stroke. Proc Natl Acad Sci U S A 2004;101:12730–12735.
33 Bergers G, Brekken R, McMahon G et al. Matrix metalloproteinase-9 triggers the angiogenic switch during carcinogenesis. Nat Cell Biol 2000;2:737–744.
34 Heissig B, Hattori K, Dias S et al. Recruitment of stem and progenitor cells from the bone marrow niche requires MMP-9 mediated release of kit-ligand. Cell 2002;109:625–637.
35 Cheng XW, Kuzuya M, Nakamura K et al. Mechanisms underlying the impairment of ischemia-induced neovascularization in matrix metalloproteinase 2-deficient mice. Circ Res 2007;100:904–913.
36 Renault MA, Losordo DW. The matrix revolutions: Matrix metalloproteinase, vasculogenesis, and ischemic tissue repair. Circ Res 2007;100: 749–750.
37 Hashimoto G, Inoki I, Fujii Y et al. Matrix metalloproteinases cleave connective tissue growth factor and reactivate angiogenic activity of vascular endothelial growth factor 165. J Biol Chem 2002;277:36288–36295.
38 Sage EH, Reed M, Funk SE et al. Cleavage of the matricellular protein SPARC by matrix metalloproteinase 3 produces polypeptides that influence angiogenesis. J Biol Chem 2003;278:37849–37857.
39 Kupatt C, Horstkotte J, Vlastos GA et al. Embryonic endothelial progenitor cells expressing a broad range of proangiogenic and remodeling factors enhance vascularization and tissue recovery in acute and chronic ischemia. FASEB J 2005;19:1576–1578.
40 Young PP, Vaughan DE, Hatzopoulos AK. Biologic properties of endothelial progenitor cells and their potential for cell therapy. Prog Cardiovasc Dis 2007;49:421–429.

See www.StemCells.com for supplemental material available online.

Downloaded from www.StemCells.com at Briscoe Library-Serials Department on March 22, 2009

A Novel Stem Cell Source for Vasculogenesis in Ischemia: Subfraction of Side Population Cells from Dental Pulp

Koichiro Iohara, Li Zheng, Hiroaki Wake, Masataka Ito, Junichi Nabekura, Hideaki Wakita, Hiroshi Nakamura, Takeshi Into, Kenji Matsushita and Misako Nakashima

Stem Cells 2008;26;2408-2418; originally published online Jun 26, 2008;
DOI: 10.1634/stemcells.2008-0393

This information is current as of March 22, 2009

Updated Information & Services	including high-resolution figures, can be found at: http://www.StemCells.com/cgi/content/full/26/9/2408
Supplementary Material	Supplementary material can be found at: http://www.StemCells.com/cgi/content/full/2008-0393/DC1

Downloaded from www.StemCells.com at Brasee Library-Serials Department on March 22, 2009

AlphaMed Press

Supplemental Material can be found at:
http://www.jbc.org/cgi/content/full/M704913200/DC1

THE JOURNAL OF BIOLOGICAL CHEMISTRY VOL. 283, NO. 6, pp. 3385–3391, February 8, 2008
Printed in the U.S.A.

Neurotrophic Factor Neurotrophin-4 Regulates Ameloblastin Expression via Full-length *TrkB*[*] [S]

Received for publication, June 14, 2007, and in revised form, October 31, 2007 Published, JBC Papers in Press, November 28, 2007, DOI 10.1074/jbc.M704913200

Keigo Yoshizaki[‡§], Shinya Yamamoto[‡], Aya Yamada[‡], Kenji Yuasa[‡], Tsutomu Iwamoto[‡], Emiko Fukumoto[¶], Hidemitsu Harada[‖], Masahiro Saito[**], Akihiko Nakasima[§], Kazuaki Nonaka[‡], Yoshihiko Yamada[‡‡], and Satoshi Fukumoto[‡§§1]

From the Section of [‡]Pediatric Dentistry and [§]Orthodontics, Division of Oral Health, Growth, and Development, Faculty of Dental Science, Kyushu University, Fukuoka 812-8582, Japan, [¶]Nagasaki University Graduate School of Biomedical Sciences, Nagasaki 852-8521, Japan, the [‖]Department of Oral Anatomy II, Iwate Medical College School of Dentistry, Morioka, Iwate 020-8505, Japan, the [**]Department of Molecular and Cellular Biochemistry, Osaka University Graduate School of Dentistry, Suita, Osaka 565-0871, Japan, the [‡‡]Craniofacial Developmental Biology and Regeneration Branch, NIDCR, National Institutes of Health, Bethesda, Maryland 20892, and the [§§]Division of Pediatric Dentistry, Department of Oral Health and Development Sciences, Tohoku University Graduate School of Dentistry, Sendai, Miyagi 980-8575, Japan

Neurotrophic factors play an important role in the development and maintenance of not only neural but also nonneural tissues. Several neurotrophic factors are expressed in dental tissues, but their role in tooth development is not clear. Here, we report that neurotrophic factor neurotrophin (NT)-4 promotes differentiation of dental epithelial cells and enhances the expression of enamel matrix genes. Dental epithelial cells from 3-day-old mice expressed NT-4 and three variants of *TrkB* receptors for neurotrophins (full-length *TrkB-FL* and truncated *TrkB-T1* and *-T2*). Dental epithelial cell line HAT-7 expressed these genes, similar to those in dental epithelial cells. We found that NT-4 reduced HAT-7 cell proliferation and induced the expression of enamel matrix genes, such as ameloblastin (Ambn). Transfection of HAT-7 cells with the *TrkB-FL* expression construct enhanced the NT-4-mediated induction of Ambn expression. This enhancement was blocked by K252a, an inhibitor for *Trk* tyrosine kinases. Phosphorylation of ERK1/2, a downstream molecule of *TrkB*, was induced in HAT-7 cells upon NT-4 treatment. *TrkB-FL* but not *TrkB-T1* transfection increased the phosphorylation level of ERK1/2 in NT-4-treated HAT-7 cells. These results suggest that NT-4 induced Ambn expression via the *TrkB*-MAPK pathway. The p75 inhibitor TAT-pep5 decreased NT-4-mediated induction of the expression of Ambn, *TrkB-FL*, and *TrkB-T1*, suggesting that both high affinity and low affinity neurotrophin receptors were required for NT-4 activity. We found that NT-4-null mice developed a thin enamel layer and had a decrease in Ambn expression. Our results suggest that NT-4 regulates proliferation and differentiation of the dental epithelium and promotes production of the enamel matrix.

Mammalian development is a complex and highly orchestrated process that involves intricate cross-talk between growth factors and other regulatory molecules. The interaction between the epithelium and mesenchyme induces specific molecular and cellular changes that lead to organogenesis. These interactions are particularly crucial during the initiation of the development of ectodermal organs, such as teeth, skin, hair, and mammary and prostate glands (1). The oral epithelium provides the initial signaling for neuronal crest-derived ectomesenchyme development, and then both tissues interact during tooth formation. Various transcription factors, growth factors, and extracellular matrices are expressed by enamel matrix-producing ameloblasts during tooth development (2–4). The principal components of the enamel matrix that are synthesized by secretory ameloblasts can be classified into two major categories, amelogenin (Amel)[2] and non-Amel, which includes ameloblastin (Ambn) and enamelin (Enam) (5). Ambn, also known as amelin or sheathlin, is a tooth-specific glycoprotein that represents the most abundant non-Amel enamel matrix protein. We previously created Ambn-null mice, which develop severe enamel hypoplasia in which ameloblasts detached from the matrix, lost cell polarity, resumed proliferation, and formed multiple cell layers (6). These results suggest that Ambn is essential for ameloblast differentiation and enamel formation.

Nerve growth factor (NGF), brain-derived neurotrophic factor (BDNF), and neurotrophin-3 and -4/5 (NT-3 and NT-4/5, respectively) are structurally and functionally related and belong to the neurotrophin family, which promotes the development and survival of the vertebrate nervous system (7). Neurotrophins interact with two classes of cell surface receptors. The first class is *Trk* tyrosine kinase receptors that bind neurotrophins with a high affinity (8). *TrkA* mediates the biological

[*] This work was supported in part by Grants-in-aid for Research Fellows 15689025, 17689058, 19791585, and 17659650 from the Japan Society for the Promotion of Science and the Ministry of Education, Science, and Culture of Japan (to S. F., A. Y., and K. N.). The costs of publication of this article were defrayed in part by the payment of page charges. This article must therefore be hereby marked "*advertisement*" in accordance with 18 U.S.C. Section 1734 solely to indicate this fact.

[S] The on-line version of this article (available at http://www.jbc.org) contains supplemental Table 1 and Figs. 1–3.

To whom correspondence should be addressed: Division of Pediatric Dentistry, Dept. of Oral Health and Development Sciences, Tohoku University Graduate School of Dentistry, Sendai, Miyagi 980-8575, Japan. Fax: 81-22-717-8380; E-mail: fukumoto@mail.tains.tohoku.ac.jp.

[2] The abbreviations used are: Amel, amelogenin; BrdUrd, bromo-2′-deoxyuridine; MAPK, mitogen-activated protein kinase; ERK, extracellular signal-regulated kinase; Ambn, ameloblastin; Enam, enamelin; NGF, neural growth factor; BDNF, brain-derived neurotrophic factor; NT, neurotrophin; PBS, phosphate-buffered saline; RT, reverse transcriptase; MEK, mitogen-activated protein kinase/extracellular signal-regulated kinase kinase; P1, P3, and P7, postnatal day 1, 3, and 7, respectively.

Downloaded from www.jbc.org at OSAKA UNIVERSITY on March 5, 2008

response of NGF, *TrkC* is activated by NT-3, and BDNF and NT-4/5 are the preferred ligands for *TrkB* (7). *TrkB* and *TrkC* have truncated transcripts at the C terminus (9–12). The second class is the common low affinity neurotrophin receptor, p75, which does not have a tyrosine kinase domain (13, 14). Further, neurotrophins have other regulatory roles during embryogenesis. NGF is a mitogenic factor for human epithelial cells (15), and NT-3 stimulates the proliferation of migratory neural crest cells (16). The expression of p75 may be required for kidney morphogenesis (17) and also promote apoptosis (18, 19). In the skin, the expression of BDNF and NT-4 is strikingly dependent on the hair cycle and peaks during spontaneous, apoptosis-driven hair follicle regression, known as catagen. NT-4 was also reported to accelerate catagen development in murine skin organ cultures. These results suggest that NT-4 is useful as an agent of hair growth control.

During tooth development, neurotrophic factors and their receptors are expressed in the tooth germ (20). However, their role in tooth development has not been elucidated. At the initiation stages of tooth germ development, NGF is expressed in the dental mesenchyme and weakly in the dental epithelium. At the bud stage, the majority of dental epithelial cells have lost their NGF expression, although NGF is still expressed in the inner dental epithelium and condensed mesenchyme. During later embryonic and early postnatal tooth development, NGF can be observed in the dental follicles. At the bell stage, NGF appears in epithelial cells of the stratum intermedium, whereas after birth it is restricted to cells located in the cervical part of the enamel organ. In the postnatal period, NGF is also detected in the dental papilla mesenchyme. BDNF is expressed in the region of developing rat teeth as well as in the mesenchyme under the developing skin of the mandibular process (20). In postnatal animals, BDNF is mainly detected in the dental papilla, and its expression pattern is correlated with the onset of dental innervation (21). NT-3 is expressed throughout the mesenchyme of the mandibular process at the initiation stage, whereas it appears in the epithelial cervical loops in the cap stage. During later stages, NT-3 expression is gradually restricted to the more cervical parts of the inner enamel epithelium and is no longer detected in postnatal tooth germs (20). The expression of NT-4 is restricted to epithelial cells. During subsequent development, expression persists in all dental epithelium components, including ameloblasts and the outer enamel epithelium as well as in the dental lamina (20, 21). Among neurotrophic factors, NT-4 is the only one detected in differentiated ameloblasts. These findings suggest that NT-4 may be important for dental epithelium differentiation and maintenance of ameloblast functions. However, the role of NT-4 in tooth development is unknown.

In the present study, we investigated the roles of NT-4 and *TrkB* in tooth development *in vitro* using dental epithelium cultures and *in vivo* using NT-4 knock-out mice. NT-4 and *TrkB* receptors were expressed in the dental epithelium of 3-day-old mice and in the HAT-7 dental epithelial cell line. We found that NT-4 inhibited proliferation and induced differentiation of HAT-7 cells. NT-4 treatment of HAT-7 cells increased mRNA expression for enamel matrix proteins Ambn, Enam, and dentin sialophosphoprotein. Further, NT-4-mediated induction of Ambn expression was regulated by the full-length *TrkB-FL* receptor and ERK1/2 pathway. In NT-4 knock-out mice, Ambn expression was dramatically reduced, and the enamel layer was thin. Our findings suggest that NT-4 plays a role in proliferation and differentiation of the dental epithelium and is required for the expression of enamel matrix genes.

EXPERIMENTAL PROCEDURES

Cell Culture and Transfection—HAT-7 cells, an epithelial cell line, and mDP cells, a dental mesenchymal cell line, were maintained in Dulbecco's modified Eagle's medium/F-12 medium supplemented with 10% fetal bovine serum and 1% penicillin and streptomycin at 37 °C in a humidified atmosphere containing 5% CO_2 (22). To transfect with the expression vectors for *TrkB*, HAT-7 cells were plated in a 60-mm plastic tissue culture plate (Falcon) at a density of 1×10^6 cells/3 ml/plate. To facilitate the detection of protein expression, V5 and His tags were fused to the C terminus of the two rat *TrkB* isoforms, *TrkB-FL* and *TrkB-T1*. *TrkB-FL* and *TrkB-T1* cDNA were prepared from adult rat brain mRNA by RT-PCR and confirmed by DNA sequencing. The forward primer for *TrkB-FL* and *TrkB-T1* was 5′-CTCTGACTGACTGGCACTGG-3′, and the reverse primer was 5′-GCCTAGGATGTCCAGGTAGACGGGC-3′ for *TrkB-FL* or 5′-CCCATCCAGGGGGATCTTA-3′ for *TrkB-T1*. PCR was performed at 94 °C for 30 s, 60 °C for 30 s, and 72 °C for 60 s for 30 cycles. The PCR products were cloned into pEF6/V5-His-TOPO® (Invitrogen) according to the manufacturer's protocol. Cells were transfected using Lipofectamine 2000 (Invitrogen) according to the manufacturer's protocol. Stable transfectant cells for *TrkB-FL* and *TrkB-T1* were selected in the presence of 5 μg/ml Blasticidin (Invitrogen).

Cell Proliferation and Bromodeoxyuridine (BrdUrd) Incorporation—Cells were plated at 1×10^5 cells/ml/well in 12-well plates for 24 h. Cell numbers were determined using a trypan blue dye exclusion method. For the BrdUrd incorporation assay, cells were incubated at the same cell density described above for 24 h prior to the addition of various growth factors. After treatments with various growth factors, BrdUrd (Sigma) was added to the plates (10 μM) for 30 min, and then the cells were fixed with cold methanol for 10 min, rehydrated in phosphate-buffered saline (PBS), and incubated for 30 min in 1.5 M HCl. After washing three times in PBS, the plates were incubated with a 1:50 dilution of fluorescein isothiocyanate-conjugated anti-BrdUrd antibody (Roche Applied Science) for 30 min at room temperature. Finally, the cells were washed in PBS three times and incubated with 10 μg/ml propidium iodide (Sigma) in PBS for 30 min at room temperature. BrdUrd-positive cells were examined under a microscope (Biozero-8000; Keyence, Japan).

Western Blotting—Cells were plated in 12-well plates at 1×10^5 cells/well for 1 day prior to NT-4 treatment. The cells were then treated with 100 ng/ml NT-4 for 0–60 min at 37 °C. Thereafter, they were washed twice with ice-cold 1 mM sodium orthovanadate (Sigma) in PBS, lysed with Nonidet P-40 buffer supplemented with a proteinase inhibitor mixture (Sigma) and phenylmethanesulfonyl fluoride at 4 °C for 10 min, and centrifuged, and then the supernatants were transferred to a fresh

tube. The cell lysates were separated by 12% SDS-PAGE and analyzed by Western blotting. The blotted membrane was incubated with antibodies, and the signals were detected with an ECL kit (Amersham Biosciences). ERK and second antibodies were purchased from Cell Signaling.

RNA Isolation and RT-PCR—Developing molars were dissected from mice on postnatal day 1 (P1), P3, and P7. Epithelial and mesenchymal tissues were separated from tooth germ from P3 mice under a microscope. Total RNA was isolated using TRIzol (Invitrogen) according to the manufacturer's protocol. First strand cDNA was synthesized at 42 °C for 90 min using oligo$(dT)_{14}$ primer with SuperScript III (Invitrogen). PCR amplification was performed using the primers listed in supplemental Table 1. The PCR products were separated on a 1.5% agarose gel. The relative expression level was deduced from a standard curve constructed using the positive control sample and normalized against the expression level of HPRT in each sample.

Protein Kinase-inhibitory Assay—Serum-deprived HAT-7 cells were plated in 6-well plates and treated with 0.5 μM K-252a (*Trk* tyrosine kinase inhibitor; Calbiochem) and 100 nM TAT-Pep5 (p75NTR signaling inhibitor; Calbiochem) prior to treatment with NT-4 for 30 min. After 48 h, total RNA was extracted, and RT-PCR was performed.

Preparation of Tissue Sections and HE Staining—Mouse heads from P1, P3, and P7 wild-type and NT-4 null mice were fixed with 4% paraformaldehyde in PBS overnight at 4 °C. The tissues were decalcified with 250 mM EDTA/PBS for 3 days, dehydrated in xylene through a graded ethanol series, and then embedded in paraffin. Sections were sliced at 8 μm using a microtome (RM2125RT; Leica). For detailed morphological analysis of the molars, the sections were stained with Harris hematoxylin (Sigma) and Eosine Y (Sigma). The widths of enamel matrix and dentin were measured under a microscope (Bisozero-8000).

RESULTS

Expression of NT-4 and TrkB Receptors in the Tooth Germs and Dental Cell Lines—We first examined the expression of NT-4 and *TrkB* receptors in tooth germs and dental cell lines by RT-PCR. In tooth germs of P3 mice, NT-4 was highly expressed in the dental epithelium and weakly expressed in the dental mesenchyme (Fig. 1*A*). The full-length *TrkB-FL* and truncated *TrkB-T1* and *-T2* were expressed in the dental epithelium. On the other hand, *TrkB-T1*, but not *TrkB-FL* or *TrkB-T2*, was expressed in the mesenchyme. Further, p75 expression levels were low in both the epithelium and mesenchyme (Fig. 1*A*). The expression patterns of NT-4, *TrkB*s, and p75 in dental epithelial cell line HAT-7 and dental mesenchyme cell line mDP were similar to those in the tooth germ tissues, except for a low expression level of *TrkB-FL* in mDP cells and a high expression level of p75 in HAT-7 cells (Fig. 1*B*). These results suggest that NT-4, *TrkB-FL*, *TrkB-T1*, and *TrkB-T2* are expressed in the dental epithelium and may regulate differentiation of the dental epithelium.

Inhibition of Proliferation of HAT-7 Cells by NT-4—We next examined the effect of NT-4 on HAT-7 cell proliferation (Fig. 2). HAT-7 cells were treated with NT-4, and cell proliferation was analyzed by BrdUrd incorporation for 1 h. The number of

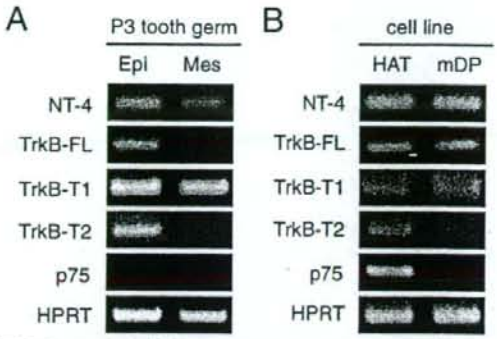

FIGURE 1. **Expression of NT-4 and receptors in tooth germs and dental cell lines.** Tooth germs were dissected from P3 mice, and the dental epithelium (*Epi*) and mesenchyme (*Mes*) were separated under a microscope. Total mRNA from these tissues was amplified using a semiquantitative RT-PCR method with specific primer sets (*A*). Total mRNA expression of NT-4 and *TrkB* receptors in dental epithelial cell line HAT-7 and mesenchymal cell line mDP was analyzed by RT-PCR (*B*).

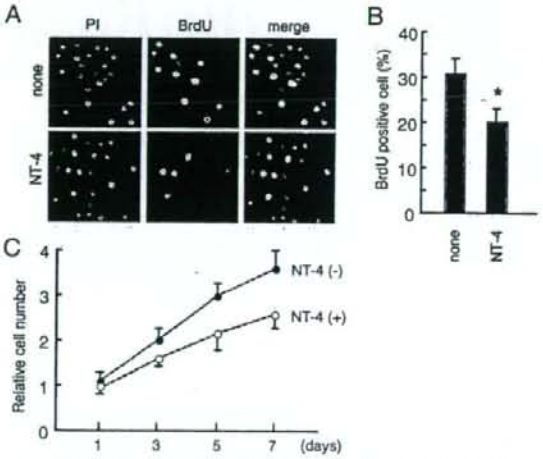

FIGURE 2. **NT-4 inhibits cell proliferation.** Dental epithelial cells (HAT-7) were cultured with NT-4 for 24 h. BrdUrd incorporation after 1 h was analyzed using a fluorescence microscope (*A* and *B*). Cell numbers of HAT-7 cells cultured with or without NT-4 were counted using a trypan blue exclusion method after 1, 3, 5, and 7 days of culture (*C*). These experiments were repeated at least five times with similar results. Statistical analysis was performed using analysis of variance (*, $p < 0.01$).

BrdUrd-positive cells was decreased by 30% after stimulation with NT-4 (Fig. 2, *A* and *B*). We also found that the number of HAT-7 cells was decreased by about 25% when the cells were cultured in the presence of NT-4 for 7 days (Fig. 2*C*). These results indicate that NT-4 inhibits the proliferation of dental epithelial cells in culture.

NT-4 Induces Ambn Expression—To analyze the effects of neurotrophic factors on dental epithelium differentiation, NGF, BDNF, or NT-4 was added to HAT-7 cell cultures. After 48 h, total RNA was analyzed for the expression of ameloblast differentiation markers by RT-PCR. Ambn, Enam, dentin sialophosphoprotein (*Dspp*), osteopontin (*Opn*), and osteonectin (*Osn*) were induced by NGF, BDNF, and NT-4 (Fig. 3, *A* and *B*).

Downloaded from www.jbc.org at OSAKA UNIVERSITY on March 5, 2008